



HAL
open science

Separation of complex branched polymers by size-exclusion chromatography probed with multiple detection

Marianne Gaborieau, Julien Nicolas, Maud Save, Bernadette Charleux, Jean-Pierre Vairon, Robert G Gilbert, Patrice Castignolles

► To cite this version:

Marianne Gaborieau, Julien Nicolas, Maud Save, Bernadette Charleux, Jean-Pierre Vairon, et al.. Separation of complex branched polymers by size-exclusion chromatography probed with multiple detection. *Journal of Chromatography A*, 2008, 1190 (1-2), pp.215-223. 10.1016/j.chroma.2008.03.031 . hal-04085489

HAL Id: hal-04085489

<https://hal.science/hal-04085489>

Submitted on 29 Apr 2023

HAL is a multi-disciplinary open access archive for the deposit and dissemination of scientific research documents, whether they are published or not. The documents may come from teaching and research institutions in France or abroad, or from public or private research centers.

L'archive ouverte pluridisciplinaire **HAL**, est destinée au dépôt et à la diffusion de documents scientifiques de niveau recherche, publiés ou non, émanant des établissements d'enseignement et de recherche français ou étrangers, des laboratoires publics ou privés.



Distributed under a Creative Commons Attribution - NonCommercial - NoDerivatives 4.0 International License

1 Separation of complex branched polymers by size-exclusion 2 chromatography probed with multiple detection

3 *Marianne Gaborieau,^{1,2} Julien Nicolas,^{3,4} Maud Save,³ Bernadette Charleux,³ Jean-*
4 *Pierre Vairon,³ Robert G. Gilbert,¹ Patrice Castignolles*^{1,3}*

5 ¹ *Centre for Nutrition and Food Sciences, Hartley Teakle Building, The University of Queensland,*
6 *Brisbane, QLD 4072, Australia*

7 ² *Max Planck Institute for Polymer Research, Ackermannweg 10, D-55128 Mainz, Germany*

8 ³ *Laboratoire de Chimie des Polymères – UMR 7610, Université P. et M. Curie, 4 Place Jussieu,*
9 *75252 Paris, Cedex 05, France*

10 ⁴ *Permanent address : Laboratoire de Physico-Chimie, Pharmacotechnie et Biopharmacie, UMR*
11 *CNRS 8612, Univ Paris-Sud, Faculté de Pharmacie, 5 rue Jean-Baptiste Clément, 92296 Châtenay-*
12 *Malabry, France*

13 *p.castignolles@uq.edu.au*

14 *Prepared for submission to Journal of Chromatography, A.*

15 **Abstract:**

16 Size-exclusion chromatography (SEC) separates polymers by hydrodynamic volume (the
17 universal calibration principle). Molecular weights can be determined using viscometry (relying on
18 universal calibration) and light scattering (independent of universal calibration). In the case of
19 complex branched polyacrylates with tetrahydrofuran as eluent, universal calibration is valid,
20 although the separation in term of molecular weight is incomplete: a given elution slice contains a
21 range of molecular weights, described in terms of a ‘local polydispersity’. The local polydispersity
22 index decreases when the number of branches per chain increases and complete separation is
23 reached for highly branched chains.

24 **Keywords:** Multiple-detection Size-exclusion Chromatography (SEC), separation, polyacrylate,
25 complex branched polymer, molecular weight, hydrodynamic volume

26 **Introduction**

27 Size-exclusion chromatography (SEC) is a technique widely used to analyze
28 synthetic and natural polymers [1,2]. These polymers have a distribution of molecular weights
29 (MW). Branched polymers constitute an important class of polymers, which can be divided in two
30 main categories: (a) regularly-branched polymers (e.g. regular stars, combs, dendrimers, H, pom-
31 pom polymers etc.[3]), in which all polymeric chains have the same number of branches and the
32 branches have the same size for each chain; (b) complex branched polymers, in which there is a
33 distribution of number of branches and/or size of the branches. Branching is present in several
34 important families of polymer: (i) starch, the major component of human nutrition [4], also
35 extensively used industrially [5]; (ii) glycogen, another energy storage polysaccharide [6]; (iii)

36 polyethylene, the most widely produced synthetic polymer, which is statistically branched when
37 produced by free-radical polymerization [7]; (iv) poly(vinyl acetate), extensively used for paints
38 and adhesives [8] and (v) polyacrylates, with numerous applications for coatings and pressure-
39 sensitive adhesives [9]. Furthermore, all monomers polymerizable by chain polymerization can
40 form complex branched polymers if copolymerized with a difunctional monomer (see e.g. [10,11]).
41 Another family of interesting complex branched polymers comprises dendritic ones [12], but these
42 will not be further considered in the present context. This work deals with statistically branched
43 homopolymers: the case of copolymers, whose chemical heterogeneity can be another source of
44 complexity, or the case of non-statistical branching are not treated here.

45 It is well known, but often unappreciated by practitioners, that even under ideal conditions,
46 SEC separates polymer chains by their hydrodynamic volume V_h (universal calibration principle),
47 but not by their MW. The validity of universal calibration for the separation of complex branched
48 polymers has been the object of successive controversies in the literature. Wild and Guliana [13]
49 studied fractionated polyethylene samples by SEC, viscometry, osmometry and light scattering.
50 They observed that different calibration curves ($\log M = f(t_{el})$, where t_{el} is the elution time) were
51 obtained for SEC of linear and long-chain branched polymers and concluded that long-chain
52 branching plays a role in the SEC separation. Benoit *et al.* [14-16] demonstrated for a range of
53 polymers that for each t_{el} , the product of intrinsic viscosity $[\eta]$ by molecular weight M is
54 independent of the nature of the polymer, which constitutes the universal calibration in SEC. In
55 practice, they measured weight-average intrinsic viscosity $[\eta]_w$ and weight-average molecular
56 weight \bar{M}_w of linear and different types of branched (comb, star) narrow standards, obtained by
57 living anionic polymerization and/or fractionation. Universal calibration has been proved to be valid
58 for many other polymers, e.g. polyethylene [13,17], poly(ethylene oxide) [18], polysaccharides
59 [18,19], polypeptides [20], globular proteins [19], and hyperbranched polymers when the end-
60 groups are have no significant interactions with the stationary phase [21,22]. The use of the product
61 $[\eta]_w \cdot \bar{M}_w$ to apply universal calibration was disproved by Hamielec *et al.* [8,23-25] in the case of
62 statistically branched poly(vinyl acetate). Their experimental results and theoretical treatment
63 proved that universal calibration is actually valid for statistically branched polymers using the
64 product $[\eta]_w \cdot \bar{M}_n$, where \bar{M}_n is the number-average molecular weight. When the separation obeys
65 a size-exclusion mechanism, a given t_{el} always corresponds to a single value of the product
66 $[\eta]_w \cdot \bar{M}_n$, which has dimensions of molar volume and is the functional definition the hydrodynamic
67 volume V_h .

68 As made clear by Hamielec and coworkers, complex branched polymers elute in SEC into
69 fractions which are polydisperse in terms of MW even though they possess the same V_h [8,23-25].
70 The presence of more than one type of polymer molecule at a particular t_{el} has been termed
71 “imperfect resolution” [24], “structural polydispersity” [11] or more generally “local
72 polydispersity” [2,26]. Local polydispersity is generally assumed to be negligible [11,27]. Mueller
73 *et al.* [21] proved the absence of local polydispersity in the SEC of hyperbranched poly(methyl
74 methacrylate) using multiple detection. Balke *et al.* [28] characterized complex branched polymers
75 by universal calibration together with low-angle laser light scattering (LALLS). They compared the
76 three methods then available in the literature: chromatogram comparison, conventional calibration
77 and universal calibration. This permitted the detection of the local polydispersity for some samples,
78 but no quantification. All of these methods require the use of a linear equivalent of the branched
79 sample. Synthesizing a linear equivalent over an appropriate range of MW may be expensive, time-
80 consuming or even impossible, for example in the case of amylopectin. Furthermore, comparison
81 methods are time-consuming. For a complex branched polymer, there can be a distribution of
82 chains with different MWs but the same V_h . The separation will thus be incomplete even if

83 universal calibration is valid. Hence, SEC of a complex branched polymer cannot, even in principle,
84 yield a molecular weight distribution (MWD), irrespective of whatever battery of online detectors
85 may be employed.

86 SEC separation of some complex polymers has been claimed to be disturbed by anomalous
87 elution behavior: the molecular weight determined by multi-angle light scattering (MALLS) at each
88 t_{el} decreases with t_{el} , as expected, but then increases at higher t_{el} [29]. This was observed for star
89 copolymers of styrene and butadiene [30], copolymers of styrene and divinyl benzene [30-32],
90 heparin [33], dendritic polymers [34] and polymacromonomers [35]. It was also observed for linear
91 chains, polystyrene (see figure 2 of [36]), poly(styrene sulfonate) (see figure 23 of [37]) and
92 polyesters[38]. In the case of polyesters, the anomalous behavior is observed only when
93 determining the molecular weight by MALLS but not with a determination by triple detection
94 (combining right-angle laser light scattering and viscometry). Contradictory observations have been
95 given for this effect such as the suppression of microgels because the presence of a precolumn may
96 [30] or may not [32] mask anomalous elution behavior. Anomalous elution behavior is indeed not
97 observed for hyperbranched poly(methyl methacrylate) analyzed by viscometry (relying on
98 universal calibration) as well as light scattering [21,29]. Burchard *et al.*[6] also observed this
99 anomalous behavior of the determined molecular weight against t_{el} with SEC MALLS of glycogen;
100 however, they showed by successive degradation of glycogen that this effect is purely an artifact
101 due to data treatment. Calibration curves $\log M$ against t_{el} are meaningful only in the range where
102 light scattering and refractometer signals are intense enough (in terms of signal-to-noise ratio). This
103 has been proved by simulating SEC MALLS results including noise on the refractometer and
104 MALLS detector signals [39]. At high t_{el} , at which the actual signal intensities are low, the noise
105 induces the generation of successively negative and positive values of MW. However, these data
106 are fitted as $\log M$ by commonly used software and the logarithm of a negative number is not
107 defined; such software thus replaces the negative values by zero before fitting. $\log M$ values are then
108 overestimated, even if a proper size-exclusion mechanism takes place. Note that the input
109 chromatograms used to simulate “anomalous elution” (as shown by the refractometer and MALLS
110 traces in figure 2 of [39]) seem to exhibit very little noise.

111 A summary of the literature on multiple-detection SEC of complex branched polymers
112 follows. First, “anomalous elution” has been assigned to artifacts during data treatment and not due
113 to branching. Second, conditions where universal calibration is valid for complex branched
114 polymers have been found with a potential significant local polydispersity as demonstrated by the
115 pioneering work from Hamielec. Local polydispersity indices significantly higher than unity have
116 never been reported. Comparison of the molecular weight versus t_{el} determined both with
117 viscometry (relying on universal calibration) and light scattering is particularly valuable to reveal
118 the mechanism of separation of complex polymers [21,29]. Very few studies combine state-of-the-
119 art detection, viscometry and light scattering, together with appropriate data treatment to study the
120 separation of complex branched polymers.

121 The mechanism of separation of complex branched polyacrylates by SEC is studied in this
122 work using multiple-detection and a novel data treatment. Both viscometry and light scattering
123 detectors are used and the molecular weights against t_{el} so determined are carefully compared. The
124 aim of this article is first to investigate whether universal calibration is valid for the separation of
125 complex branched polyacrylates. When universal calibration is valid, the mechanism of separation
126 is then further examined, since complex branched polymers have not only a distribution of
127 molecular weights (MW) but also distributions of long-chain branch lengths and topologies.

128 **Experimental section**

129 *Polymerizations*

130 Materials for polymerization and polymerization conditions are fully described in the
131 supporting information. Poly(2-ethylhexyl acrylate) was synthesized by photopolymerization using
132 a pulsed laser as described previously [40]. A 1-mL solution of 2-ethylhexyl acrylates/toluene 50/50
133 wt% was polymerized to a monomer conversion of 2.7 % (gravimetry). The amount of polymer was
134 too small to allow determination of branching level by NMR, but poly(*n*-butyl acrylate) produced
135 under similar conditions (pulsed UV lamp) were measured by ¹³C solid-state NMR to contain 0.3 %
136 of branches per monomer unit [41]. Poly(ethyl acrylate) and poly(methyl acrylate) were produced
137 by conventional free-radical polymerization as a 4.7 mol·L⁻¹ monomer solution in toluene to 99 %
138 monomer conversion (gravimetry) [42]. ¹³C NMR measurements were done in CDCl₃ at 125 MHz,
139 with a 10 s relaxation delay and 20 000 transients, at 33 °C for PMA and 25 °C for PEA. They
140 showed that respectively 2.1 ± 0.5 and 1.6 ± 0.5 % of the monomeric units are branched, not
141 distinguishing between long- and short-chain branching [42]. The relative insensitivity of the
142 solution-state NMR was overcome by the use of solid-state NMR,[42] inspired by a work by
143 Klimke et al. [43]. Two poly(*n*-butyl acrylate)s were obtained by nitroxide-mediated radical
144 polymerization. High conversion poly(*n*-butyl acrylate) was obtained by miniemulsion
145 polymerization targeting high MW (theoretical \overline{M}_n of 1.07 × 10⁵ g·mol⁻¹, 88 % conversion).
146 Another poly(*n*-butyl acrylate) sample was obtained by bulk polymerization targeting low MW
147 (2.52 × 10⁴ g·mol⁻¹, 80 % conversion). Two poly(*n*-butyl acrylate)s were a generous gift from
148 Prof. Axel H.E. Mueller (University of Bayreuth) and were synthesized by anionic polymerization
149 in THF in presence of lithium 2-methoxyethoxide as a ligand [44].

150 *SEC set-up*

151 Molecular weights for polyacrylates were determined with a Viscotek triple-detector SEC set-
152 up composed of an online degasser, pump, manual injector, one precolumn and three columns (two
153 mixed-C and one 10² Å, particle size of 5 μm) from Polymer Lab., the TDA (triple detector array,
154 including in series RALLS (right-angle laser light scattering), LALLS at 7° (laser wavelength 670
155 nm), refractometer and finally viscometer), and Trisec[®] 2000 software. The software corrects for
156 inter-detector delay and makes partial correction for band broadening; the related constants are
157 given in the supporting information (Table 3) but the theory used by the software is not given by the
158 supplier. The eluent was THF at 40 °C and 1 mL·min⁻¹. Toluene was used as a flow rate marker. As
159 recommended by Coote and Davis [45], the injection loop was calibrated by weighing with toluene:
160 its volume was 53.6 μL (arithmetic mean from 3 values: 53.1, 55.5 and 52.3 μL). The different
161 detectors were calibrated injecting different polystyrene standards (PSS and Viscotek, Supporting
162 Information Table 1 and 2, molecular weight at the peak and weight-average molecular weight were
163 provided by the suppliers) of known concentration to calculate the mass constant of the
164 refractometer, the constant of the viscometer and constants for each of the two light scattering
165 detectors. On each day of use, the SEC set-up was checked using polystyrene, poly(methyl
166 methacrylate) or poly(*n*-butyl acrylate) standards (Supporting Information). Eluent alone was
167 regularly injected to check that the baseline of all the detectors, including light scattering, remained
168 flat and that thus no bleeding of the columns could change the signal of the online detectors.

169 The dn/dc values used in this work were either determined using the refractometer or
170 extrapolated from the literature in the case of poly(*n*-butyl acrylate) (see Supporting Information).

171 All averaging of curves, fits, etc. were carried out using Origin® software. In this work an
172 online viscometer was used and thus the Mark-Houwink-Sakurada relation was not needed.

173 *Optimization of multiple-detector SEC to reduce noise (case of polyacrylates)*

174 It is important to optimize the concentration of the injected polymer to obtain low-noise
175 chromatograms when using multiple-detector SEC. The uncertainty arising from the determination
176 of the concentration by the refractometer will affect the determination of the intrinsic viscosity by
177 the viscometer and/or the determination of the molecular weight by light scattering. This problem is
178 enhanced by the difference in sensitivity between the refractometer, a mass-sensitive detector, and
179 the molecular-weight sensitive detectors (viscometer or light scattering). The refractometer has a
180 poorer sensitivity for high MWs and a higher sensitivity for low MWs than the molecular-weight
181 sensitive ones. This explains for example some so-called “anomalous elution” behavior [6].
182 Optimizing the injection concentration in the case of polyacrylates is even more important because
183 of their low refractive index increment dn/dc (around $0.06 \text{ dL} \cdot \text{g}^{-1}$ in THF, Supporting Information).
184 Using the following empirical relation, the concentration C_{\max} to be injected was calculated as [46]:

$$185 \quad C_{\max} = \frac{0.2}{[\eta] \cdot V_{\text{inj}}} \quad (1)$$

186 where C_{\max} is in $\text{g} \cdot \text{L}^{-1}$, the intrinsic viscosity $[\eta]$ is in $\text{dL} \cdot \text{g}^{-1}$ and the injected volume V_{inj} is in mL.
187 Note the unusual units of this empirical relation implying that the constant 0.2 includes a correction
188 factor (10^4) for converting volumes into L and has dimension of volume (L). To prevent any
189 overloading of the columns, we chose to work at concentrations of ca $C_{\max}/2$ (typically 1 to $10 \text{ g} \cdot \text{L}^{-1}$).
190 The resulting raw chromatograms had low noise (Fig. 1). They also give a qualitative indication
191 of the presence of long-chain branching: for the very high MWs (several million $\text{g} \cdot \text{mol}^{-1}$,
192 corresponding to the exclusion limit of the columns) at very low t_{el} , a very intense peak appears on
193 the light scattering trace while nearly no signal can be detected by the refractometer. The same
194 types of chromatograms have been observed for long-chain branched polyethylene [47].

195 Note that the determination of the concentration by the refractometer is still valid with
196 statistically branched systems, since dn/dc has been shown not to vary with branching level [48].
197 The analysis of complex branched polymers by multiple-detection SEC is easier than that of
198 copolymers with composition distributions; in the latter case, dn/dc indeed usually varies with
199 composition.

200 Even working at the optimal injection concentration, the MWDs determined from these
201 chromatograms are still very noisy (Fig. 2, gray line). Note that the highest level of noise lies on the
202 y-axis, $w(\log M)$, since this is calculated using the refractometer trace divided by the slope of the
203 calibration curve, $\log M = f(t_{\text{el}})$ [49]. The Trisec® software available with the device used here only
204 allows the determination of MWDs via a regression fitting of the $\log M$ against t_{el} for one sample at
205 a time. With our samples, this leads to very poor fits (Fig. 3 top). An improved method of data
206 treatment is as follows. Instead of smoothing the data, Bruessau [50] recommends repeating the
207 analysis several times and co-adding the chromatograms. Since we use a triple-detector SEC, we
208 decided not to co-add the chromatograms but instead to co-add the $\log M = f(t_{\text{el}})$ obtained from these
209 chromatograms. First, Trisec® is used to obtain the $\log M = f(t_{\text{el}})$ from the chromatograms of single
210 injections using either universal calibration, triple detection or LALLS. It is assumed here that
211 samples of the same monomer polymerized over the same narrow ranges of temperature ($\pm 5^\circ\text{C}$)
212 and monomer concentration ($\pm 0.5 \text{ mol} \cdot \text{L}^{-1}$) will have similar branching distributions. The $\log M =$

213 $f(t_{el})$ curves for all these polymers are plotted together and the total data set fitted by a polynomial.
214 The arithmetic mean is thus calculated before the fit (Fig. 3 bottom). Fitting the $\log M = f(t_{el})$ curves
215 for several samples brings two benefits: it reduces the noise, especially at the limit volumes on both
216 sides, and the $\log M = f(t_{el})$ plot can be obtained over a broad range of MW by putting together
217 samples having different MW ranges. The fit yields the calibration curve subsequently used to treat
218 the refractometer chromatograms via a classical conventional calibration with Trisec[®]. The
219 distribution so obtained is much less noisy (Fig. 2).

220 This two-step data treatment appears important for the determination of average MWs even in the
221 case of linear polymers. Indeed, to obtain meaningful MWs in multiple-detector SEC and avoid so-
222 called “anomalous elution” behavior, the integration limits have to be restricted to that part of the
223 chromatogram where all the detectors yield a significant signal to prevent random number
224 generation (i.e. number whose uncertainty becomes larger than the number itself) at low and high t_{el}
225 (corresponding to very weak signals with the refractometer and with the MW sensitive detectors
226 respectively) [51]. These integration limits would thus yield an overestimate of \bar{M}_n (the integration
227 limit at high t_{el} cuts out some oligomers) and an underestimate of \bar{M}_w (the integration limit at low
228 t_{el} cuts out the highest molecular weight) [50], and thus an underestimate of their ratio, the
229 polydispersity $I_p = \bar{M}_w / \bar{M}_n$. Our two-step approach makes it possible to constrain the integration
230 limits to a reasonable range to calibrate the columns using multiple-detection SEC. In the second
231 step, conventional calibration is used with broad integration limits corresponding to the full
232 refractometer signal for the whole polymer, including for example a low-MW tail where the light
233 scattering signal is low.

234 **Results and discussion**

235 *Comparison of the molecular weights determined by viscometry (relying on universal calibration)* 236 *and light scattering using multiple-detection SEC*

237 Multiple-detector SEC set-ups allow MWs to be determined by two independent techniques:
238 viscometry (relying on universal calibration) and light scattering (LALLS or triple detection or
239 MALLS). These techniques should yield the same MWs, and this is indeed seen within
240 experimental error for all analyzed standards, which are linear chains: polystyrene, poly(methyl
241 methacrylate) and poly(*n*-butyl acrylate) (Supporting Information and Fig. 4). The standards
242 synthesized by anionic polymerization, polystyrene, poly(methyl methacrylate) and two poly(*n*-
243 butyl acrylate) samples (Fig. 4 b), are likely to be linear chains, since no branching or transfer to
244 polymer has been reported in the literature with this polymerization method [52]. Analogs of the
245 poly(*n*-butyl acrylate) produced by controlled free-radical polymerization (Fig. 4a) were studied by
246 MALDI TOF MS, which detected short-chain branching but no long-chain branching [53]. Short-
247 chain branching has a very limited effect on the V_h as long as only a few percent of the monomer
248 units are branched [54]. The results obtained with the standards prove that the SEC set-up is well
249 calibrated, and also that universal calibration is valid with the columns, eluent and poly(alkyl
250 acrylates) used here.

251 When statistically branched polyacrylates were analyzed, the MW obtained from universal
252 calibration was significantly lower than that from the LS-based techniques. In the case of
253 polyacrylates, three different free-radical polymerization processes were compared: PLP,
254 conventional free-radical polymerization and nitroxide-mediated controlled free-radical
255 polymerization. The same samples were injected several times and the raw $\log M$ against t_{el} are
256 presented in Fig. 5. Differences in the $\log M$ against t_{el} determined by viscometry/universal

257 calibration and light scattering-based methods have so far been reported only twice in the literature
258 by Hofe in the case of SEC of polyisocyanates in hexane [55] and by Mourey (nature of the
259 polymer not specified) [29]. The difference between MWs determined by universal calibration and
260 light scattering can be due to non-size-exclusion effects, i.e. adsorption effects. The recovery is thus
261 an important parameter: for polyisocyanates in hexane, it is low, as only 30-50 % of the injected
262 polymer is detected. The mechanism of separation is thus certainly not a pure size-exclusion one
263 and universal calibration is not valid in these conditions in hexane. In the case of the polyacrylates
264 analyzed in this work, THF is an appropriate solvent for SEC separation of flexible polyacrylates,
265 since recovery was measured to be quantitative. The difference between MWs could also be due to
266 the presence of microgels. However, the microgels would affect the MWs determined at the lowest
267 elution volume and the difference is not significant at these elution volumes. Furthermore,
268 microgels are obtained by intermolecular transfer to polymer combined with termination by
269 combination. The amount and nature of microgels likely differs significantly among the three
270 different polymerization process used in this work, but the difference in MWs is qualitatively the
271 same for all the samples.

272 *Why does universal calibration yield lower molecular weights than light-scattering based*
273 *techniques?*

274 The difference between MW determined by universal calibration and triple detection is absent for
275 linear chains and systematic for branched acrylic polymers and thus very likely arises in this case
276 from the presence of distributions of lengths of long-chain branches and of number of branches per
277 chain in this case. Each elution slice then contains a range of molecular weights, as in the
278 “incomplete separation” in terms of MW observed for statistically branched poly(vinyl acetate) by
279 Hamielec *et al.* [8,23,25] At a given t_{el} , a mixture of chains of different MWs will be detected. In-
280 line viscometry yields the local weight-average intrinsic viscosity and this value used together with
281 the universal calibration curve yield the number-average MW of this iso- V_h distribution: $\overline{M}_n(V_h)$
282 [8,23,25,49]. On the other hand, every light-scattering-based method will yield a weight-average
283 MW of this iso- V_h distribution: $\overline{M}_w(V_h)$ [8][56][49]. This is consistent with our experimental
284 observation that universal calibration yields lower MWs than triple detection ($\overline{M}_n(V_h) < \overline{M}_w(V_h)$).
285 Note that the average MWs for the iso- V_h distribution are completely different from the average
286 MWs for the whole MWD: $\overline{M}_n(V_h) \neq \overline{M}_n$ and $\overline{M}_w(V_h) \neq \overline{M}_w$. The measurement of the
287 dependence of both $\overline{M}_n(V_h)$ and $\overline{M}_w(V_h)$ on V_h makes it possible to measure the local
288 polydispersity index $I_p(V_h) = \overline{M}_w(V_h) / \overline{M}_n(V_h)$ [24,25]. Experimental values of $I_p(V_h)$ are reported
289 for the first time in this work. The values for the different polyacrylates studied are given in Fig. 6
290 and some are significantly higher than unity, as predicted by Hamielec *et al.* [8] Thus local
291 polydispersity is not always negligible. The values, up to 2.5, are reasonable when one considers
292 that at a given intrinsic viscosity, the molecular weight can change by several orders of magnitude
293 depending on branching (up to 2 orders of magnitude for copolymer of methyl methacrylate and
294 ethylene glycol dimethacrylate [10]).

295 *Validity of the local polydispersity observed for slightly long-chain branched polyacrylates*

296 The occurrence of a local polydispersity was predicted by Hamielec *et al.* [25] and proved
297 by some of the present authors [49] through a rigorous derivation of the form of the response from
298 different SEC detectors. The occurrence of an artifact due to unknown technical issues was ruled
299 out by applying several consistency checks: (i) high polydispersity is observed for different types of
300 samples produced by conventional free-radical polymerization (Fig. 6a), controlled radical

301 polymerization (Fig. 6b) and pulsed laser polymerization (Fig. 5c); (ii) linear polymers, even of the
302 same chemical nature, do not exhibit such a polydispersity (Fig. 4); (iii) the same results were
303 obtained with the same SEC set-up but over an extended period of time using different calibrations
304 for the detectors and the columns (Supporting Information). The SEC columns used in this work
305 yielded a good separation (an internal test was the regular analysis of multimodal samples produced
306 by pulsed laser polymerization [57]).

307 MALDI ToF mass spectrometry used as an offline or online detector [58] might, in
308 principle, provide another means to measure the local polydispersity index. However, MALDI ToF
309 mass spectrometry suffers from bias in molecular weight and thus cannot be used to measure
310 polydispersity [58,59] unless this were close to unity. MALDI ToF mass spectrometry would
311 underestimate the local polydispersity index and is thus unlikely to confirm or disprove the
312 occurrence of local polydispersity. Fractionation by SEC is generally used to overcome the bias in
313 MALDI ToF MS, but in the case of our complex branched polymers, the fractionation gives
314 insufficient separation in molecular weight to avoid this bias.

315 Under similar conditions to those used for polyacrylates (complex branched polymers,
316 constant dn/dc , Fig. 5 d), Balke *et al.* [26] predicted a different behavior: the difference between
317 universal calibration and LALLS would decrease with t_{el} , if universal calibration is valid. The
318 difference with our results (Fig. 5 a, b and c) can be explained by the branching distributions. Balke
319 injected polyesters obtained by a different process, namely polycondensation, and the branching
320 distribution is obviously different from that obtained by a free-radical polymerization process.

321 The observation that local polydispersity index $I_p(V_h)$ can be significantly greater than unity
322 could also be due to band broadening, even in the case of linear chains [25]. However, as previously
323 stated, this effect has been partially corrected by the Trisec® software and is not observed for
324 polymer standards (Fig. 4 and Supporting Information). This is generally the case with modern high
325 resolution columns [28].

326 The theory of determination of MW by triple detection has been described previously
327 [38,49,60]. This determination involves calculating the form factor iteratively using the following
328 equation to approximate the radius of gyration, R_g : [3,60]

329
$$R_g = \frac{1}{\sqrt{6}} \left(\frac{[\eta]M}{\Phi} \right)^{1/3} \quad (2)$$

330 where Φ is the Flory-Fox coefficient. The local polydispersity leads an underestimation of the form
331 factor calculated by triple detection [49]. The MW determined by triple detection is thus an
332 overestimate of the expected $\bar{M}_w(V_h)$. However, it has been shown that polydispersity has a little
333 influence on the value of the form factor [61] compared to the difference observed between $\bar{M}_n(V_h)$
334 and $\bar{M}_w(V_h)$ observed on a wide range of V_h . The measured local polydispersity index could also be
335 overestimated because of the increase up to a factor 2 of the Flory-Fox coefficient with the
336 branching and MW of the polymers [3,62]. Note however that the Flory-Fox coefficient is not used
337 here for universal calibration, but is used to calculate MW by the triple detection method. However,
338 it is used for higher MW (lower t_{el}), when the form factor becomes less than unity and RALLS
339 (right-angle laser light scattering) alone can no longer be used for MW determination. RALLS
340 consists of determining the MW using the Rayleigh equation together with the single 90° angle
341 assuming a value of unity for the form factor. If the value of the Flory-Fox coefficient had a

342 significant negative impact on the MW determined by triple detection, then triple detection and
343 universal calibration would agree at lower MWs (high t_{el}) and differ at higher MWs, i.e. the
344 measured polydispersity $I_p(V_h)$ would increase with V_h (decrease with t_{el}). However, the contrary is
345 experimentally observed. Second, the Flory-Fox coefficient is not used in the LALLS calculation,
346 and LALLS and triple detection agree within experimental error, giving a second proof that the
347 effect of the value of the Flory-Fox coefficient on the calculation of the local polydispersity is
348 negligible compared to that of the actual local polydispersity of the sample. Note that the values of
349 radius of gyration are not given in this work. They cannot be determined by LALLS or triple
350 detection. Values of radius of gyration can be calculated from the molecular weight values and
351 equation (2); however, these values cannot bring any additional information because of the validity
352 of equation (2) and the value of the Flory-Fox discussed above and because their qualitative
353 behavior against elution time has to be the same as MWs.

354 Separation of ultrahigh molecular weight polymers often suffers from molecular
355 degradation, viscous fingering etc. [63]. However, none of the samples analyzed in this work
356 contain a significant amount of ultrahigh molecular weights. The local polydispersity reach in fact
357 its highest value for the lowest molecular weights (obtained by nitroxide-mediated polymerization).
358 The highest molecular weight standards have a more pronounced tail toward elution time
359 (Supporting Information) indicating some degradation may occur for these standards due to
360 relatively high flowrate and low column particle sizes used in this work.

361 *Complete SEC separation for highly branched polyacrylates*

362 Hamielec *et al.* [25] predicted local polydispersity index to increase above unity at lower t_{el} where
363 the molecular weights are larger and the long-chain branching frequencies are higher, i.e. $I_p(V_h)$
364 should increase with V_h . Fig. 6 shows the opposite trend in the present system. This can be
365 rationalized because the number of long-chain branches per chain should increase with the chain
366 length, since long-chain branches are likely to originate from intermolecular chain transfer to
367 polymer [64,65] and the probability of this transfer reaction scales with the number of monomer
368 unit in the polymer chain, i.e with its molecular weight. Different topologies are thus obtained at
369 different V_h . At a given V_h , the difference in MW between a linear chain, a 3-arm star, a H-shaped
370 chain, etc. should be significant. When the number of branches per chain, n , is higher, i.e. for the
371 longer chains, the difference of MW between chains of the same V_h with n and $n+1$ long-chain
372 branches should become smaller [66]. This may explain why $I_p(V_h)$ decreases with increasing V_h
373 even if the number of long-chain branches per chain increases with increasing V_h . Further
374 investigation is needed to confirm this explanation. While the influence of regular branching in SEC
375 is well understood and has been successfully modeled [67], the situation of complex branched
376 polymers is far less understood and far more complex because of the change of the branching
377 topology and distribution of length of the branches with V_h . Note $I_p(V_h)$ increase when the
378 branching level decrease as long as some chains are branched; in the case of linear (or regular-
379 branched) homopolymers, there is a one-to-one relation between MW and V_h and thus $I_p(V_h)$ is
380 unity, i.e. the separation is complete in terms of MW (assuming no band-broadening). If one could
381 plot $I_p(V_h)$ against average branching level for a given type of polymer on a given experimental set-
382 up, a discontinuity should thus been observed.

383 The mechanism of separation is important for the detection of long-chain branching. The
384 separation of complex branched polymers by SEC is indeed more sensitive to a small average
385 number of long-chain branches per chain (leading to a mixture of significantly different topologies)
386 than to a high one (leading to similar topologies). Thus, the averaged local polydispersity index is
387 higher for slightly branched polyacrylate produced by PLP at low conversion or nitroxide-mediated
388 controlled free-radical polymerization at high conversion (Fig. 6 b) than for a highly-branched

389 polyacrylate produced by conventional free-radical polymerization at high conversion (Fig. 6a).
390 While nitroxide-mediated controlled free-radical polymerization generally yields polyacrylates with
391 significantly less than one long-chain branch per chain (Fig. 4a and reference [53]), targeting high
392 MW ($1.07 \times 10^5 \text{ g} \cdot \text{mol}^{-1}$) leads to more branches per chain and then high local polydispersity index
393 up to 2.5 (Fig. 5b). The local polydispersity index is lower, below 1.5 when a polyacrylate which
394 may contain more long-chain branches per chain is measured, since it is obtained by conventional
395 free-radical polymerization. This is illustrated by Fig. 6a for poly(ethyl acrylate). The same range of
396 $I_p(V_h)$ is obtained for poly(methyl acrylate) obtained in the same conditions (data not shown [42]).
397 Increasing the long-chain branching level even more should make it thus possible to obtain a very
398 low and negligible local polydispersity index $I_p(V_h)$: on Figure 6, $I_p(V_h)$ reach values very close to
399 unity at highest V_h , i.e. highest long-chain branching levels for polyacrylates.

400 This is also consistent with the Mark-Houwink plots observed with low density
401 polyethylene (LDPE) [13] or branched polystyrenes [3], as follows. The mechanism of formation of
402 the branches in LDPE (free-radical polymerization) is the same as in polyacrylates: intermolecular
403 chain transfer to polymer leads to long-chain branching and the probability of long-chain branching
404 increases with the chain length. The longer the LDPE or polyacrylate chains, the higher the long-
405 chain branching level. In the case of LDPE, this has been extensively proven to lead to a curved
406 Mark-Houwink plot [13], with the intrinsic viscosity leveling off at high chain length/branching
407 level. This is consistent with our observation: for sufficiently highly branched polymers, the
408 intrinsic viscosity does not vary with MW (see the case of hyperbranched polymers [68]) and there
409 is then a one-to-one relation between V_h and MW. This one-to-one relation implies complete
410 separation of the species by SEC and thus a local polydispersity index of one as measured by
411 Mueller *et al.* for highly-branched poly(methyl methacrylate) [21]. Jackson *et al.* [27] may have
412 produced such samples using methyl methacrylate and a difunctional comonomer. They observed
413 that the \overline{M}_w s for the whole distribution obtained from offline static light scattering and SEC-
414 MALLS are in good agreement. Gnanou *et al.* [69] observed the same agreement between offline
415 static light scattering and SEC-MALLS for 7th generation dendrimer-like, and not dendrimers,
416 poly(ethylene oxide). Since offline static light scattering is not affected by local polydispersity
417 problems, one can conclude that for these samples with higher long-chain branching level, the local
418 polydispersity is low and negligible. Recent Monte Carlo simulations of hyperbranched polymers
419 [70] confirm that the local polydispersity index should be very close to unity for this type of
420 randomly hyperbranched polymer [71]. This confirms the validity of the SEC MALLS analysis of
421 glycogen, an hyperbranched polymer [6]. The literature on Mark-Houwink-Sakurada parameters of
422 polyacrylates has been reviewed,[40] but Mark-Houwink plots are not informative for the
423 polyacrylates treated here[42]. The molecular weight range may be too narrow and Mark-Houwink
424 plots exhibit noise on both axis, $\log M$ and $\log[\eta]$, and in the case of polyacrylates, low dn/dc values
425 make this noise too important.

426 The same situation might apply for the separation of the two main components of starch:
427 amylose and amylopectin, as long as universal calibration holds. Since amylopectin is highly
428 branched while amylose is slightly branched [72], the averaged local polydispersity index may be
429 higher for amylose than for amylopectin. One has however to be careful when dealing with very
430 high branching levels, as found in amylopectin or hyperbranched polymers in general. This is for at
431 least two reasons. First, the increase in the number of end-groups (chemically different from the
432 monomeric unit) with respect to the number of monomeric units might favor their interactions with
433 the stationary phase. This would change the mechanism of the separation by SEC and lead to the
434 non-validity of universal calibration when the end-groups exhibit significant enthalpic interactions.
435 This depends on both the number and nature of the end-groups [12,22]. Second, the equations used

436 to calculate the V_h and the form factor expression for triple detection or MALLS have been derived
437 for linear chains and not for complex branched polymers [49].

438 *Conclusions*

439 Complex branched polyacrylates have been separated by SEC. Multiple-detection SEC enables to
440 determine molecular weight by two independent methods: viscometry (relying on universal
441 calibration) and light scattering, and thus validate or not the size-exclusion mechanism of
442 separation. While multiple-detection SEC is a unique tool to detect even very low level of long-
443 chain branches, the use of multiple-detectors does not guarantee the determination of true molecular
444 weights and critical comparison of universal calibration and light scattering results is thus highly
445 recommended for complex polymers. Complete separation in SEC (in terms of molecular weight)
446 can be obtained for highly branched polymers if interactions with the stationary phase are
447 minimized. A true size-exclusion separation takes place for poly(alkyl acrylates) in THF but the
448 presence of a low level of long-chain branches prevents a complete separation in terms of molecular
449 weight.

450 The treatment of data obtained from the SEC separation of statistically and slightly long-chain
451 branched polyacrylates as well as the determination of the MW by multiple-detection SEC
452 techniques has been carefully examined. Multiple-detection SEC yields noisy raw molecular weight
453 distribution (MWD) and can significantly overestimate molecular weight at high t_{el} (a phenomenon
454 known as “anomalous elution” although it is most probably a data treatment problem rather than a
455 separation mechanism one). To overcome this, it is recommended to co-add and fit the data:
456 collecting all the $\log M$ against t_{el} for samples having the same branching distribution. This makes it
457 possible to accurately compare the MWs of slightly branched polyacrylates obtained by three
458 different techniques on the same sample: universal calibration, triple detection and LALLS. Triple
459 detection and LALLS appear to yield systematically higher MWs than universal calibration. This is
460 attributed to the presence of a distribution of branching topologies, which induces an incomplete
461 separation according to MW in SEC. Due to the well-known phenomenon that SEC separates by
462 size and not MW, a slice of statistically branched polymer eluting at a given elution time will
463 indeed have a distribution of MWs. The true molecular weight distribution (MWD) cannot be
464 determined by SEC in that case, even using multiple-detection. At each elution time, an average
465 MW is determined: $\overline{M}_n(V_h)$ for viscometry (relying on universal calibration) and $\overline{M}_w(V_h)$ for light
466 scattering. However, more information can be derived using multiple detection as shown
467 theoretically [49]. The local polydispersity and averaged local polydispersity indices decrease when
468 long-chain branching level increases. For highly branched polymers, the SEC separation is
469 complete in terms of molecular weight and the true molecular weight distribution can be
470 determined.

471 When true molecular weight can not be determined by SEC, comparative studies can still be
472 undertaken using hydrodynamic volume distributions,[49] as recently illustrated in the study of
473 controlled/living polymerization[73] or the mechanism of action of starch branching enzymes[74].
474 Furthermore, the number and weight average molecular weight of the whole MWD, \overline{M}_n and \overline{M}_w
475 can be determined from the hydrodynamic volume distributions and respectively the local $\overline{M}_n(V_h)$
476 and $\overline{M}_w(V_h)$ even if the MWD itself can not be determined [49]. Complete separation of slightly
477 branched polyacrylates requires two-dimensional liquid chromatography methods [75] and
478 regularly-branched polymers have been already successfully separated by this method (e.g.
479 [76,77]). Separating complex branched polymers is a major challenge for polymer separation
480 science.

481 **Acknowledgments**

482 We are indebted to Prof. A.H.E. Mueller (Bayreuth) for the gift of polyacrylate samples and also
483 fruitful discussions together with Dr. Thorsten Hofe (Mainz). The Laboratoire de Chimie des
484 Polymères and MG are grateful to Arkema for funding and supplying SG1, MAMA and DIAMS
485 and to Dr Stéphane Lepizzera for discussions about branching in polyacrylates. PC thanks Dr. Odile
486 Sepulchre for her valuable technical assistance with SEC set-up. PC thanks the Australian Research
487 Council for an International Linkage Fellowship, held at the University of Sydney. MG thanks Prof.
488 Hans W. Spiess and Prof. Manfred Wilhelm for discussions about the importance and quantification
489 of branching. We thank Prof. Manfred Schmidt and Prof. Walter Burchard for insights into
490 anomalous elution. We gratefully acknowledge the support of an ARC LIEF grant (polymer
491 characterization facility) and an ARC Discovery grant.

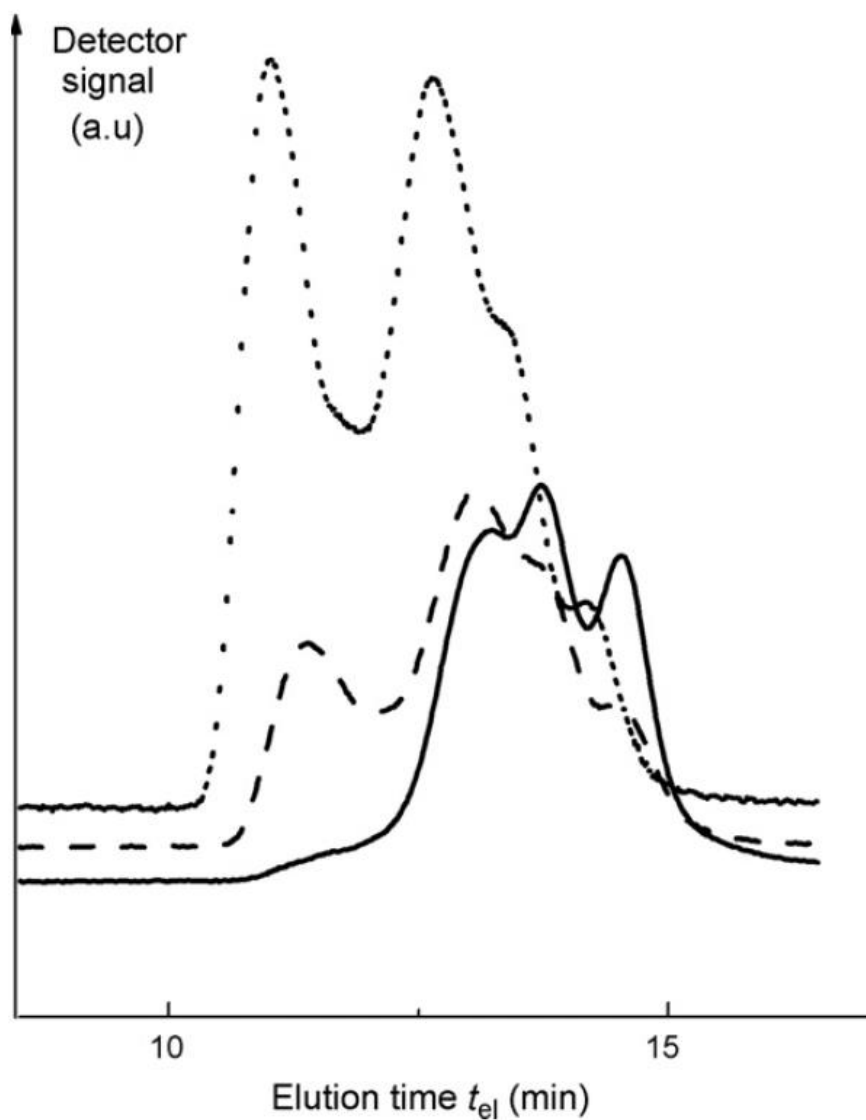
492 **References**

- 493 [1] S. Mori, H.G. Barth, Size Exclusion Chromatography, Springer-Verlag, Berlin, 1999.
- 494 [2] S.T. Balke, in H.G. Barth, J.W. Mays (Editors), Modern methods of Polymer
495 Characterization, John Wiley & Sons, New York / Chichester / Brisbane / Toronto /
496 Singapore, 1991, p. 1
- 497 [3] W. Burchard, Adv. Polym. Sci. 143 (1999) 113.
- 498 [4] M.G. James, K. Denyer, A.M. Myers, Curr. Op. Plant Biology 6 (2003) 215.
- 499 [5] J.R. Daniel, R.L. Whistler, H. Roeper, in Ullmann's Encyclopedia of Industrial Chemistry,
500 Wiley-VCH Verlag GmbH & Co. KGaA, Weinheim, 2005
- 501 [6] C.E. Ioan, T. Aberle, W. Burchard, Macromolecules 32 (1999) 7444.
- 502 [7] F.W. Billmeyer, J. Am. Chem. Soc. 75 (1953) 6118.
- 503 [8] A.E. Hamielec, A.C. Ouano, L.L. Nebenzahl, J. Liq. Chromatogr. 1 (1978) 527.
- 504 [9] E. Penzel, in Ullmann's Encyclopedia of Industrial Chemistry, Wiley-VCH Verlag GmbH
505 & Co. KGaA, Weinheim, 2005
- 506 [10] R.S. Whitney, W. Burchard, Makromol. Chem-Macromol. Chem. Phys. 181 (1980) 869.
- 507 [11] C. Degoulet, T. Nicolai, D. Durand, J.P. Busnel, Macromolecules 28 (1995) 6819.
- 508 [12] B. Voit, J. Polym. Sci. Pol. Chem. 43 (2005) 2679.
- 509 [13] L. Wild, R. Guliana, J. Polym. Sci. Part A-2 Polym. Physics 5 (1967) 1087.
- 510 [14] H. Benoit, Z. Grubisic, P. Rempp, D. Decker, J.G. Zilliox, Journal De Chimie Physique 63
511 (1966) 1507.
- 512 [15] Z. Grubisic, P. Rempp, H. Benoit, J. Polym. Sci. Part B Polym. Lett. 5 (1967) 753.
- 513 [16] Z. Grubisic, P. Rempp, H. Benoit, J. Polym. Sci. Part. B Polym. Phys. 34 (1996) 1707.
- 514 [17] E.E. Drott, R.A. Mendelson, J. Polym. Sci. Part. A-2 Polym. Phys. 8 (1970) 1373.
- 515 [18] T. Kuge, K. Kobayashi, H. Tanahashi, T. Igushi, S. Kitamura, Agricultural and Biological
516 Chemistry 48 (1984) 2375.
- 517 [19] P.L. Dubin, J.M. Principi, Macromolecules 22 (1989) 1891.

- 518 [20] E. Temyanko, P.S. Russo, H. Ricks, *Macromolecules* 34 (2001) 582.
- 519 [21] P.F.W. Simon, A.H.E. Muller, T. Pakula, *Macromolecules* 34 (2001) 1677.
- 520 [22] L. Garamszegi, T.Q. Nguyen, C.J.G. Plummer, J.A.E. Manson, *J. Liq. Chromatogr. Relat.*
521 *Technol.* 26 (2003) 207.
- 522 [23] A.E. Hamielec, A.C. Ouano, *J. Liq. Chromatogr.* 1 (1978) 111.
- 523 [24] A. Hamielec, *Pure Appl. Chem.* 54 (1982) 293.
- 524 [25] L.K. Kostanski, D.M. Keller, A.E. Hamielec, *J. Biochem. Biophys. Methods* 58 (2004) 159.
- 525 [26] T.H. Mourey, K.A. Vu, S.T. Balke, in T. Provder (Editor), *ACS Symposium series,*
526 *American Chemical Society, Washington, 1999, p. 20*
- 527 [27] C. Jackson, Y.J. Chen, J.W. Mays, *J. Appl. Polym. Sci.* 61 (1996) 865.
- 528 [28] S.T. Balke, T.H. Mourey, *J. Appl. Polym. Sci.* 81 (2001) 370.
- 529 [29] T.H. Mourey, *int. J. Polym. Anal. Ch.* 9 (2004) 97.
- 530 [30] C. Johann, P. Kilz, *J. App. Polym. Sci. App. Polym. Symp.* 48 (1991) 111.
- 531 [31] D.J. Frater, J.W. Mays, C. Jackson, *J. Polym. Sci., Part B* 1997 (1997) 141.
- 532 [32] S. Podzimek, T. Vlcek, C. Johann, *J. App. Polym. Sci.* 81 (2001) 1588.
- 533 [33] P.J. Wyatt, *Anal. Chim. Acta* 272 (1993) 1.
- 534 [34] V. Percec, C.H. Ahn, W.D. Cho, A.M. Jamieson, J. Kim, T. Leman, M. Schmidt, M. Gerle,
535 M. Moeller, S.A. Prokhorova, S.S. Sheiko, S.Z.D. Cheng, A. Zhang, G. Ungar, J.P.
536 Yeardley, *J. Am. Chem. Soc.* 120 (1998) 8619.
- 537 [35] M. Gerle, K. Fischer, S. Roos, A.H.E. Muller, M. Schmidt, S.S. Sheiko, S. Prokhorova, M.
538 Moller, *Macromolecules* 32 (1999) 2629.
- 539 [36] M.D. Zammit, T.P. Davis, *Polymer* 38 (1997) 4455.
- 540 [37] W.M. Kulicke, S. Lange, D. Heins, in T. Provder (Editor), *Chromatography of Polymers,*
541 *Hyphenated and multidimensional techniques, American Chemical Society, Washington,*
542 *1999, p. 114*
- 543 [38] M. Netopilik, P. Kratochvil, F. Schallausky, S. Reichelt, A. Lederer, *Int. J. Polym. Anal.*
544 *Charact.* 12 (2007) 285.
- 545 [39] P. Tackx, F. Bosscher, *Analytical Communications* 34 (1997) 295.
- 546 [40] L. Couvreur, G. Piteau, P. Castignolles, M. Tonge, B. Coutin, B. Charleux, J.P. Vairon,
547 *Macromol. Symp.* 174 (2001) 197.
- 548 [41] C. Plessis, G. Arzamendi, J.M. Alberdi, A.M. van Herk, J.R. Leiza, J.M. Asua, *Macromol.*
549 *Rapid Commun.* 24 (2003) 173.
- 550 [42] M. Gaborieau, Solid-state NMR investigation of spatial and dynamic heterogeneity in
551 acrylic pressure sensitive adhesives (PSAs) compared to model poly(n-alkyl acrylates) and
552 poly(n-alkyl methacrylates), PhD thesis, University Louis Pasteur, Strasbourg, France,
553 2005. <http://www-scd-ulp.u-strasbg.fr/theses/theselec.html>

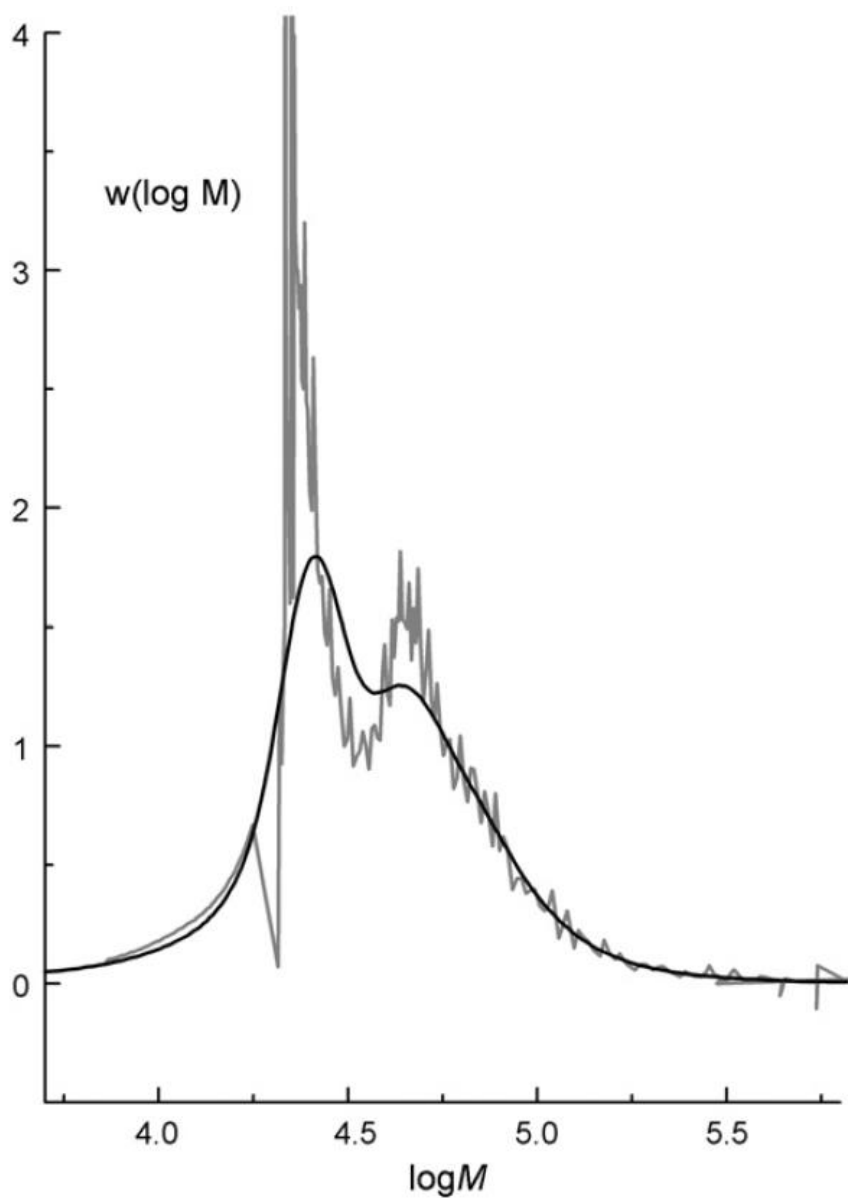
- 554 [43] K. Klimke, M. Parkinson, C. Piel, W. Kaminsky, H.W. Spiess, M. Wilhelm, *Macromol.*
555 *Chem. Phys.* 207 (2006) 382.
- 556 [44] A. Maurer, X. Marcarian, A.H.E. Muller, B. Vuillemin, C. Navarro, *Abstr. Pap. Am. Chem.*
557 *Soc.* 213 (1997) 173.
- 558 [45] M.L. Coote, T.P. Davis, *J. Polym. Sci. Pt. B-Polym. Phys.* 37 (1999) 2557.
- 559 [46] R. Mendichi, A.G. Schieroni, *J. Appl. Polym. Sci.* 68 (1998) 1651.
- 560 [47] F. Beer, G. Capaccio, L.J. Rose, *J. Appl. Polym. Sci.* 80 (2001) 2815.
- 561 [48] N. Hadjichristidis, L.J. Fetters, *J. Polym. Sci. Pt. B-Polym. Phys.* 20 (1982) 2163.
- 562 [49] M. Gaborieau, R.G. Gilbert, A. Gray-Weale, J.M. Hernandez, P. Castignolles, *Macromol.*
563 *Theory Simul.* 16 (2007) 13.
- 564 [50] R.J. Bruessau, *Macromol. Symp.* 110 (1996) 15.
- 565 [51] S. Mori, H.G. Barth, in *Size Exclusion Chromatography*, Springer-Verlag, Berlin, 1999, p.
566 120
- 567 [52] D. Baskaran, *Prog. Polym. Sci.* 28 (2003) 521.
- 568 [53] C. Farcet, J. Belleney, B. Charleux, R. Pirri, *Macromolecules* 35 (2002) 4912.
- 569 [54] T. Sun, P. Brant, R.R. Chance, W.W. Graessley, *Macromolecules* 34 (2001) 6812.
- 570 [55] T. Hofe, *Synthese und Charakterisierung von Polyisocyanaten durch GPC mit Hilfe von*
571 *molmassensensitiven Detektoren*, PhD thesis, Johannes Gutenberg University, Mainz,
572 Germany, 1997
- 573 [56] P.J. Flory, in *Principles of Polymer Chemistry*, Cornell University Press, Ithaca, New York,
574 1953, p. 266
- 575 [57] J.M. Asua, S. Beuermann, M. Buback, P. Castignolles, B. Charleux, R.G. Gilbert, R.A.
576 Hutchinson, J.R. Leiza, A.N. Nikitin, J.P. Vairon, A.M. van Herk, *Macromol. Chem. Phys.*
577 205 (2004) 2151.
- 578 [58] M.W.F. Nielen, *Mass Spectrom. Rev.* 18 (1999) 309.
- 579 [59] K. Martin, J. Spickermann, H.J. Rader, K. Mullen, *Rapid Commun. Mass Spectrom.* 10
580 (1996) 1471.
- 581 [60] D.S. Poche, R.J. Brown, L. Meiske, *J. Appl. Polym. Sci.* 85 (2002) 2178.
- 582 [61] H.J. Cantow, E. Siefert, R. Kuhn, *Chem. Ing. Tech.* 38 (1966) 1032.
- 583 [62] B.S. Farmer, K. Terao, J.W. Mays, *Int. J. Polym. Anal. Charact.* 11 (2006) 3.
- 584 [63] N. Aust, M. Parth, K. Lederer, *Int. J. Polym. Anal. Charact.* 6 (2001) 245.
- 585 [64] P.J. Flory, in *Principles of Polymer Chemistry*, Cornell University Press, Ithaca, New York,
586 1953, p. 384
- 587 [65] C. Former, J. Castro, C.M. Fellows, R.I. Tanner, R.G. Gilbert, *J. Polym. Sci. Pol. Chem.* 40
588 (2002) 3335.
- 589 [66] B.H. Zimm, *Macromolecules* 17 (1984) 2441.
- 590 [67] W. Radke, J. Gerber, G. Wittmann, *Polymer* 44 (2003) 519.

- 591 [68] R.K. Kainthan, E.B. Muliawan, S.G. Hatzikiriakos, D.E. Brooks, *Macromolecules* 39 (2006)
592 7708.
- 593 [69] X.-S. Feng, D. Taton, L. Chaikof Elliot, Y. Gnanou, *J Am Chem Soc* 127 (2005) 10956.
- 594 [70] C.J.C. Watts, A. Gray-Weale, R.G. Gilbert, *Biomacromolecules* 8 (2007) 455.
- 595 [71] D. Konkolewicz, A. Gray-Weale, R.G. Gilbert, *J. Pol. Sci. A-Polym. Chem.* 45 (2007) 3112.
- 596 [72] Y. Takeda, S. Tomooka, S. Hizukuri, *Carbohydr. Res.* 246 (1993) 267.
- 597 [73] E. Hosseini Nejad, P. Castignolles, R.G. Gilbert, Y. Guillaneuf, *J. Polym. Sci. Part A -*
598 *Polymer Chem.* in press (2008).
- 599 [74] J.M. Hernández, M. Gaborieau, P. Castignolles, M.J. Gidley, A.M. Myers, R.G. Gilbert,
600 *Biomacromolecules* accepted (2008).
- 601 [75] P.J. Schoenmakers, G. Vivo-Truyols, W.M.C. Decrop, *J. Chromatogr. A* 1120 (2006) 282.
- 602 [76] K. Im, Y. Kim, T. Chang, K. Lee, N. Choi, *J. Chromatogr. A* 1103 (2006) 235.
- 603 [77] J. Gerber, W. Radke, *e-Polymers* (2005) 12.
- 604
- 605



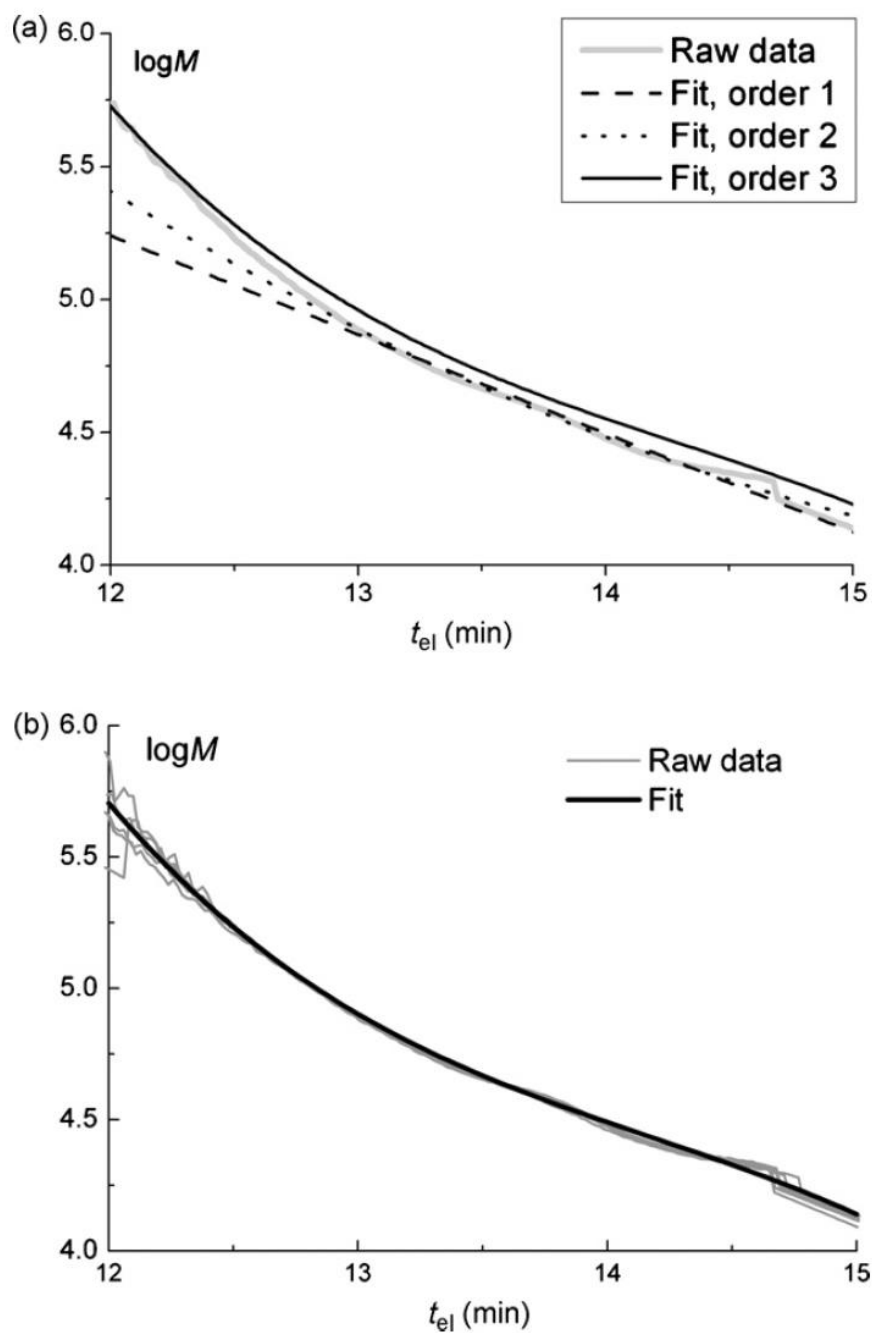
607

608 **Figure 1.** Triple-detector SEC chromatograms (raw data) of a poly(2-ethylhexyl acrylate) obtained
609 by PLP at -5°C , 100 Hz: refractometer (solid line), viscometer (dashed line), RALLS (dotted line).



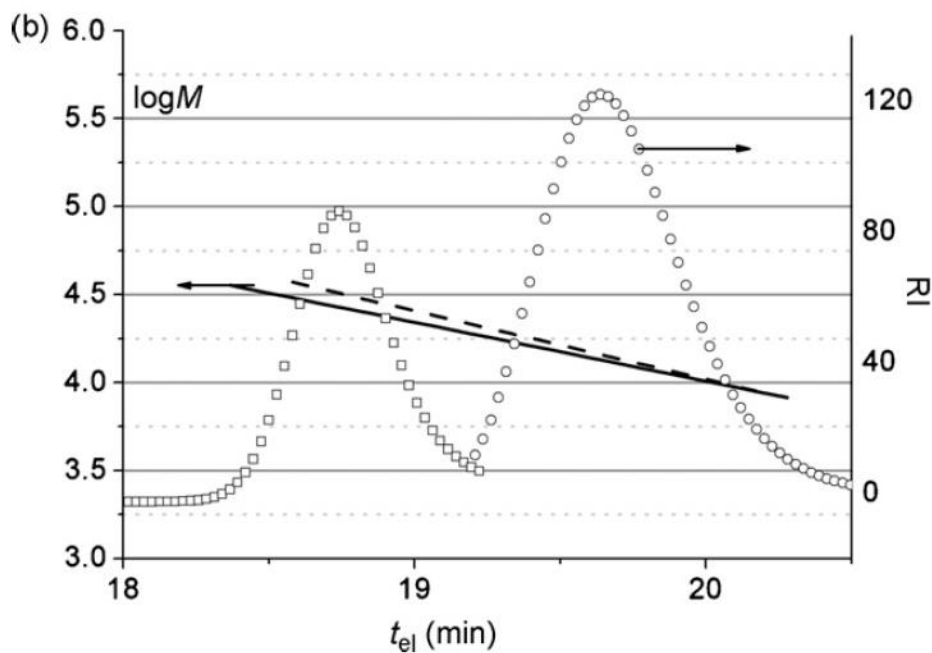
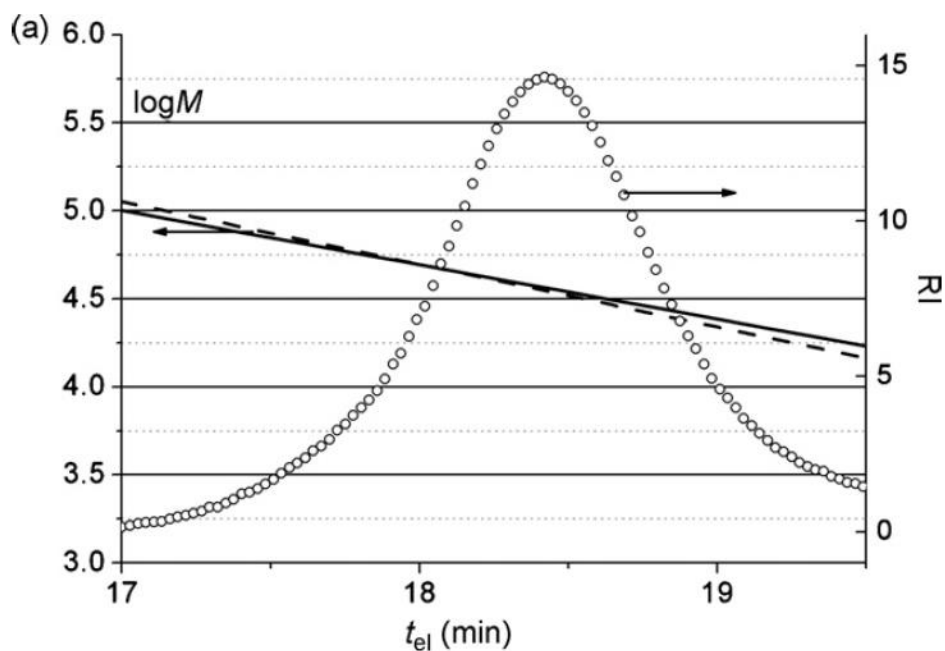
610

611 **Figure 2.** MWD obtained by Triple Detection SEC treatment (Trisec[®]) (gray line) of the
612 chromatograms of Fig. 1 and MWD obtained after fitting (black line) these data on the $\log M$ against
613 t_{el} .



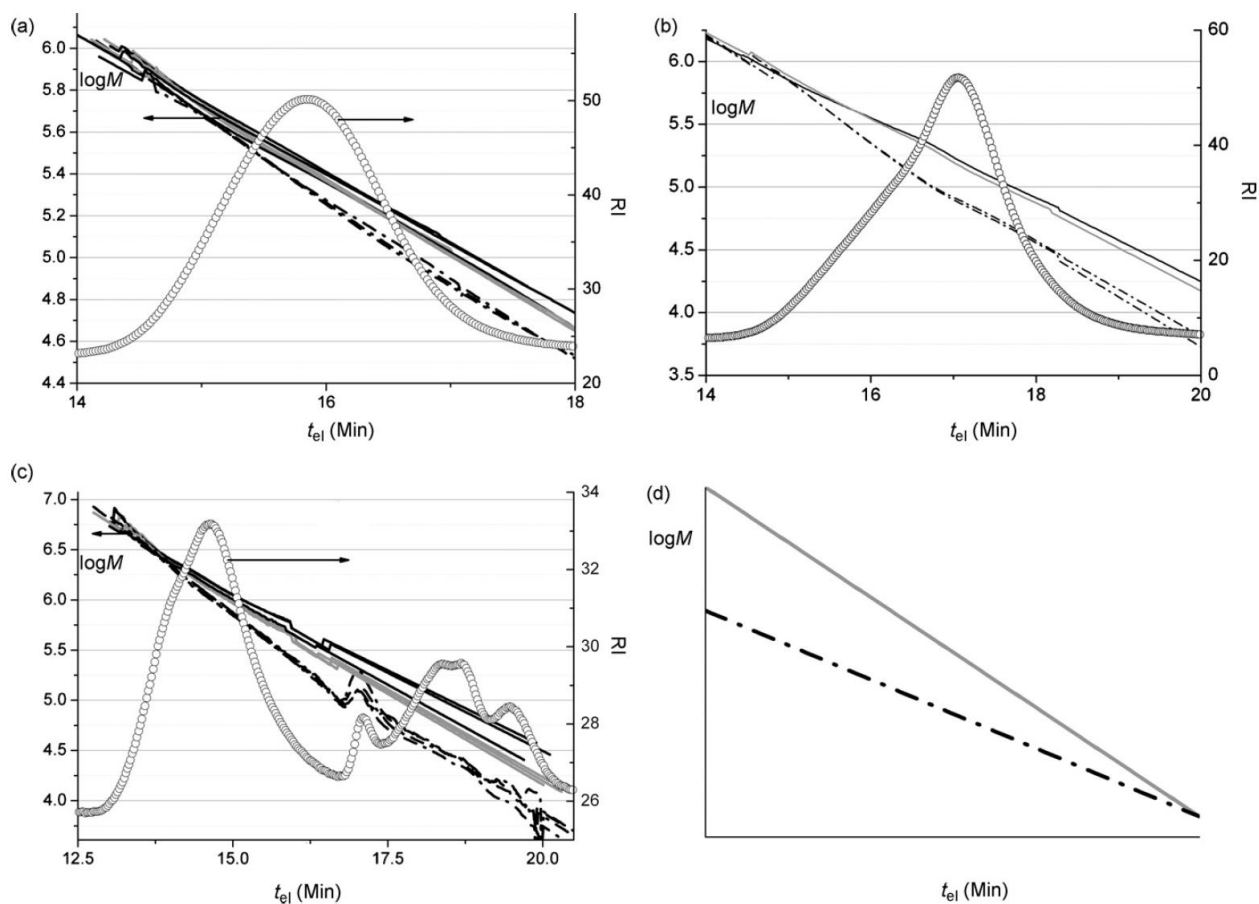
614

615 **Figure 3.** Fits of the $\log M$ against t_{el} by a polynomial (1st, 2nd and 3rd order), obtained by triple
 616 detection using Trisec[®] software for a single injection (top) and by fitting (3rd order) several
 617 injections of poly(2-ethylhexyl acrylate) obtained at the same temperature and monomer
 618 concentration (bottom).



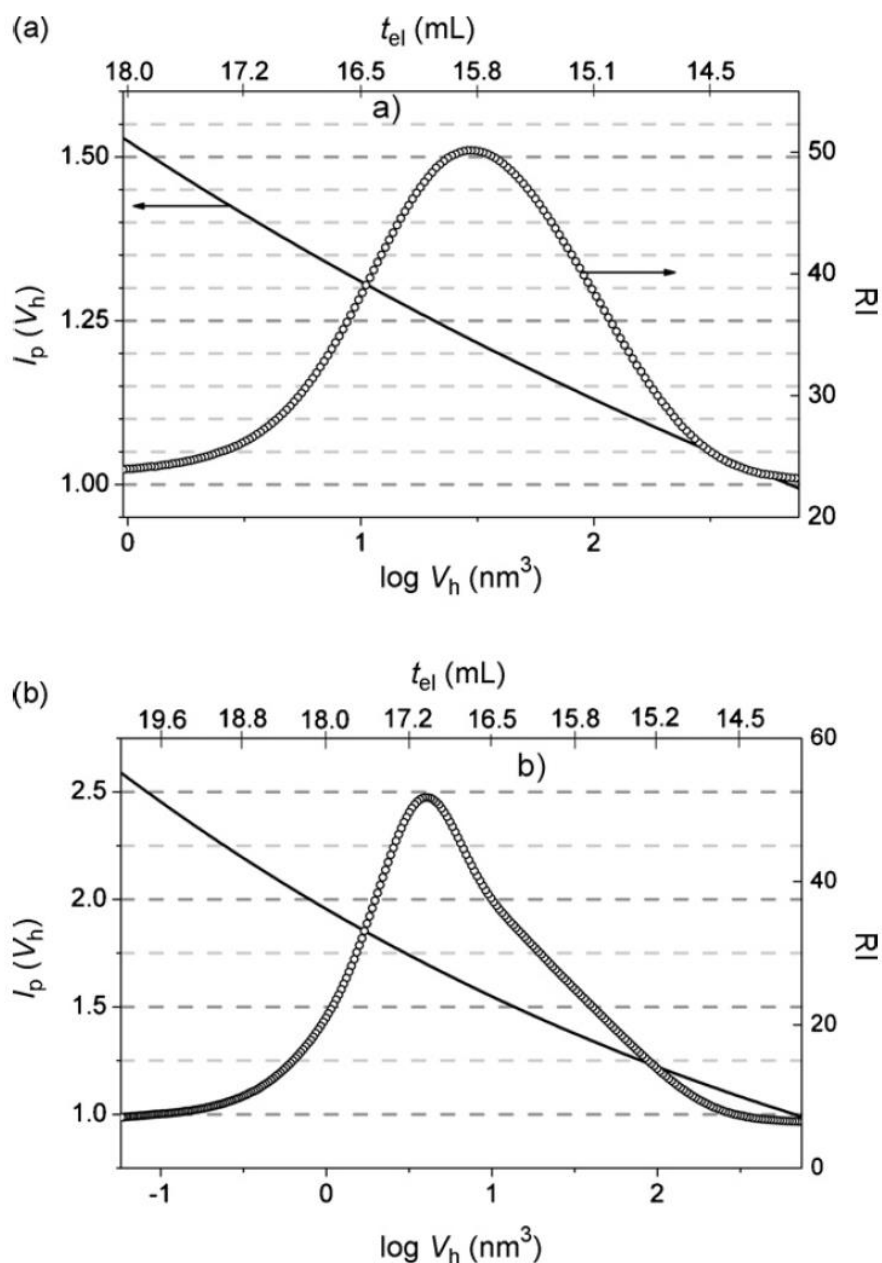
619

620 **Figure 4.** Comparison of the fit of $\log M$ against t_{el} obtained by independent methods: universal
 621 calibration (dashed line) and triple detection (solid line) for some poly(*n*-butyl acrylate) samples
 622 obtained by two different types of polymerization: nitroxide-mediated free-radical polymerization
 623 targeting low MW (a), anionic polymerization (two samples) (b). The refractometer signal is
 624 displayed with open symbols.



625

626 **Figure 5.** Comparison of the raw $\log M$ against t_{el} obtained by different methods: universal
 627 calibration (dashed dotted line), triple detection (solid gray line) and low angle laser light scattering
 628 (LALLS, solid black line) for some long-chain branched polyacrylates obtained by three different
 629 types of polymerization: conventional free-radical polymerization (poly(ethyl acrylate)) at high
 630 conversion and injected at $9.8 \text{ g}\cdot\text{L}^{-1}$ (a), nitroxide-mediated free-radical polymerization (poly(*n*-
 631 butyl acrylate) at high conversion and targeting high MW) (b), pulsed-laser polymerization (poly(2-
 632 ethylhexyl acrylate)) at low conversion (c); prediction by Balke *et al.* [26] for polymers obtained by
 633 polycondensation (d). The refractometer signal is displayed with open circles.



634

635 **Figure 6.** Variation of the local polydispersity index, $I_p(V_h)$, with hydrodynamic volume V_h for
 636 some polyacrylates obtained by different types of polymerization: conventional free-radical
 637 polymerization (poly(ethyl acrylate), Fig. 5a) (a), nitroxide-mediated free-radical polymerization
 638 (poly(*n*-butyl acrylate), Fig. 5b) targeting high MW (b). Elution time, t_{el} , has been added as top x
 639 axis to allow comparison with figure 5; note that the scale is then not linear (a third-order
 640 polynomial relation between $\log V_h$ and t_{el} has been used).

Supporting Information

Multiple-detection SEC of complex branched polyacrylates

Marianne Gaborieau, Julien Nicolas, Maud Save, Bernadette Charleux, Jean-Pierre Vairon, Robert G.

Gilbert, Patrice Castignolles*

Polymerizations

Pulsed-Laser Polymerization of 2-ethylhexyl acrylate

2-ethylhexyl (2EHA) acrylate (purity $\geq 99.5\%$, stabilized by 20 ppm of 4-methoxyphenol) was provided by Arkema, distilled under reduced pressure and systematically injected into the SEC to check the absence of preformed polyacrylates prior to use. Monomer solutions in toluene (50 wt%), containing $5 \times 10^{-3} \text{ mol}\cdot\text{L}^{-1}$ of photoinitiator (2,2-dimethoxy-2-phenylacetophenone-DMPA) (Aldrich), were carefully deoxygenated by flushing the cell with nitrogen before being submitted to laser pulses to perform photopolymerization. The photopolymerization process and laser set-up have been described previously.[1] The remaining monomer and the solvent were evaporated at room temperature and atmospheric pressure in aluminum pans before SEC analysis.

Conventional free-radical polymerization of ethyl acrylate

Ethyl acrylate (Aldrich, 99 %, stabilized with 15-20 ppm monomethyl ether hydroquinone) was distilled under reduced pressure and stored at $-20\text{ }^{\circ}\text{C}$. Ethyl acrylate was polymerized by initiating with 0.5 mol% of AIBN with respect to the acrylic monomer. The polymerization was carried out at $60\text{ }^{\circ}\text{C}$ under nitrogen for 20 h. The resulting reaction mixture was dissolved in an equal volume of dichloromethane. The polymer was then precipitated in methanol over liquid nitrogen at a temperature lower than its glass transition temperature (T_g), filtered and finally dried in an oven ($60\text{ }^{\circ}\text{C}$) under vacuum for one night. The glass transition temperature of the polymer was measured to be $-14\text{ }^{\circ}\text{C}$ by DSC at $10\text{ }^{\circ}\text{C}\cdot\text{min}^{-1}$. [2] ^{13}C NMR measurements determined that it was atactic [2].

Nitroxide-mediated free-radical polymerization of n-butyl acrylate

n-Butyl acrylate (nBA, Aldrich, 99 %) was distilled under reduced pressure before use. Dowfax 8930 and the buffer, sodium hydrogen carbonate (NaHCO_3 , Prolabo, $>99\%$) were used as received.

Hexadecane (Aldrich, $>99\%$) and high molecular weight polystyrene (Arkema, $\overline{M}_w = 330,000 \text{ g}\cdot\text{mol}^{-1}$) were also used as received. The SG1 nitroxide (86 %), the SG1-based oil-soluble dialkoxyamine, DIAMS (90 %) and the SG1-based alkoxyamine derived from methacrylic acid, MAMA (also called BlocBuilderTM, 99%), were kindly supplied by Arkema (their chemical formula are given in Figure 1).

High conversion poly(*n*-butyl acrylate) was obtained by miniemulsion polymerization, using the following method targeting high MW. A stable aqueous emulsion of nBA was prepared by mixing the organic phase with the water phase containing 406.9 g of deionized water, 2.24 g of Dowfax8390 (2.2 wt% with respect to nBA) and 0.429 g of NaHCO_3 (5.11 mmol, $12 \text{ mmol}\cdot\text{L}^{-1}_{\text{water}}$). The organic phase contained 99.57 g of nBA (0.778 mol), 0.753 g of DIAMS (0.92 mmol), 0.0076 g of free SG1 (0.026 mmol, 2.4 mol.% with respect to the alkoxyamine), 0.114 g (0.1 wt% with respect to nBA) of high MW polystyrene, 0.782 g of hexadecane (8.94 mmol, 0.8 wt% with respect to nBA). Polystyrene and hexadecane were used as hydrophobes to stabilize the monomer droplets against Ostwald ripening. The unstable emulsion formed when these components are mixed was then subjected to ultrasonication

(Branson 450 Sonifier; power 7; 10 min) in order to disperse the organic phase into submicronic droplets. This led to a stable miniemulsion, which was deoxygenated by bubbling nitrogen for 20 min at room temperature and then poured into a 600 mL glass thermostated reactor heated at 112 °C (time zero of the reaction) and stirred at 300 rpm. A 3 bar pressure of nitrogen was then applied. After 8 h of polymerization, the reactor was cooled in an iced water bath. The final latex was dried in a ventilated oven thermostated at 70 °C until constant weight. The conversion was 88 %, whence the theoretical \overline{M}_n at this conversion was 107,000 g·mol⁻¹.

Another poly(*n*-butyl acrylate) sample was obtained by bulk polymerization, using the following method targeting low MW. A mixture of the MAMA alkoxyamine (1.894 g, 4.97 mmol) and *n*-butyl acrylate (162.9 g, 1.27 mmol) was deoxygenated with nitrogen bubbling for 20 min at room temperature. The mixture was poured into a 300 mL thermostated glass reactor heated at 112 °C and stirred at 300 rpm. A 1 bar pressure of nitrogen was then applied to allow sample withdrawal. The samples were dried to measure the conversion, 80 %, by gravimetry in a ventilated oven thermostated at 70 °C until constant weight. The theoretical \overline{M}_n at this conversion was 25,200 g·mol⁻¹.

Figure 1. Chemical formula of some chemicals used in the nitroxide-mediated controlled free radical polymerization:

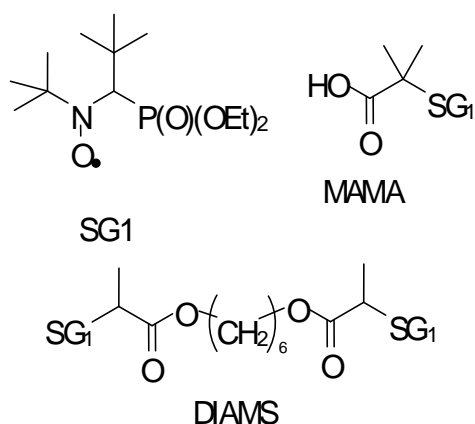
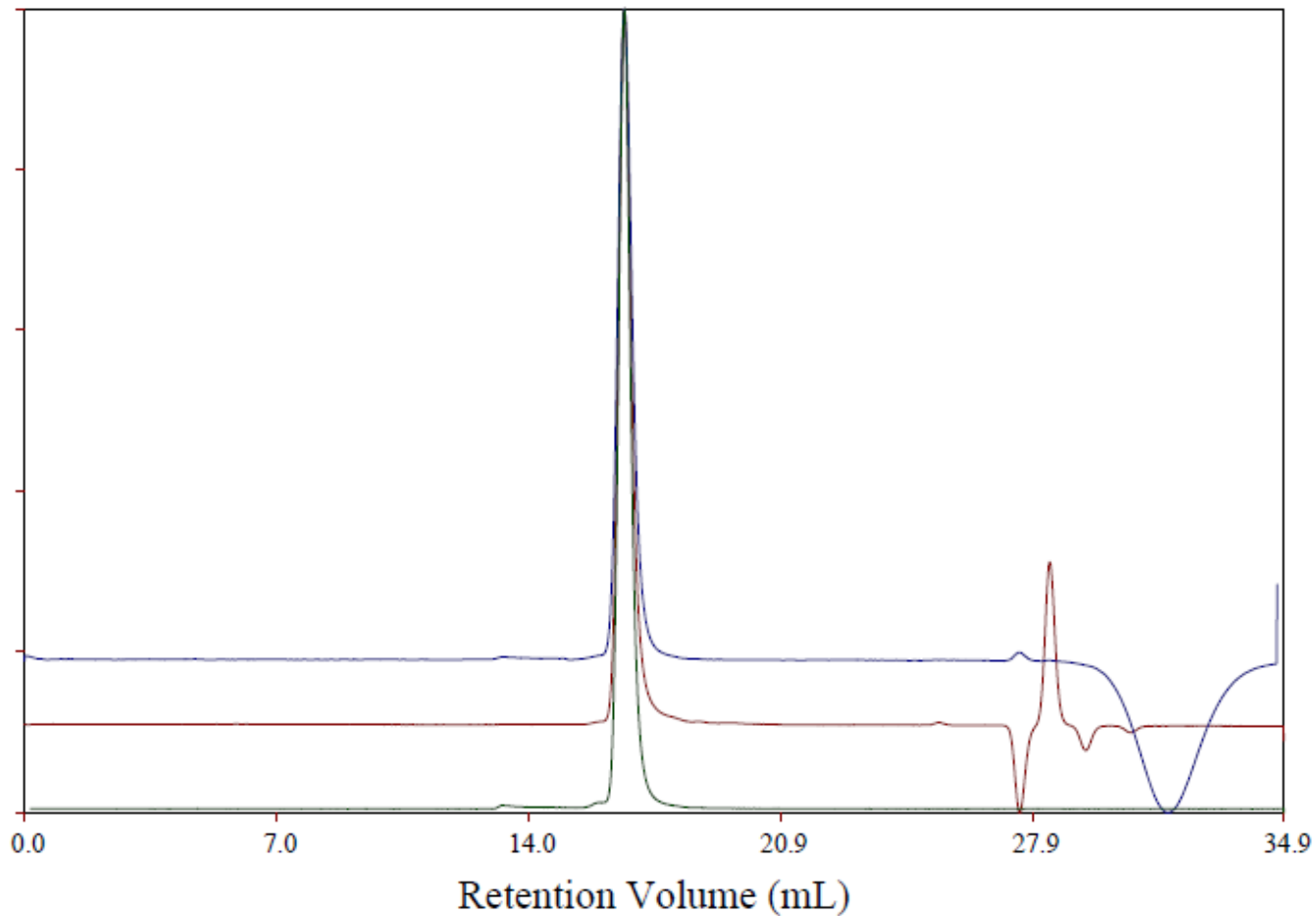
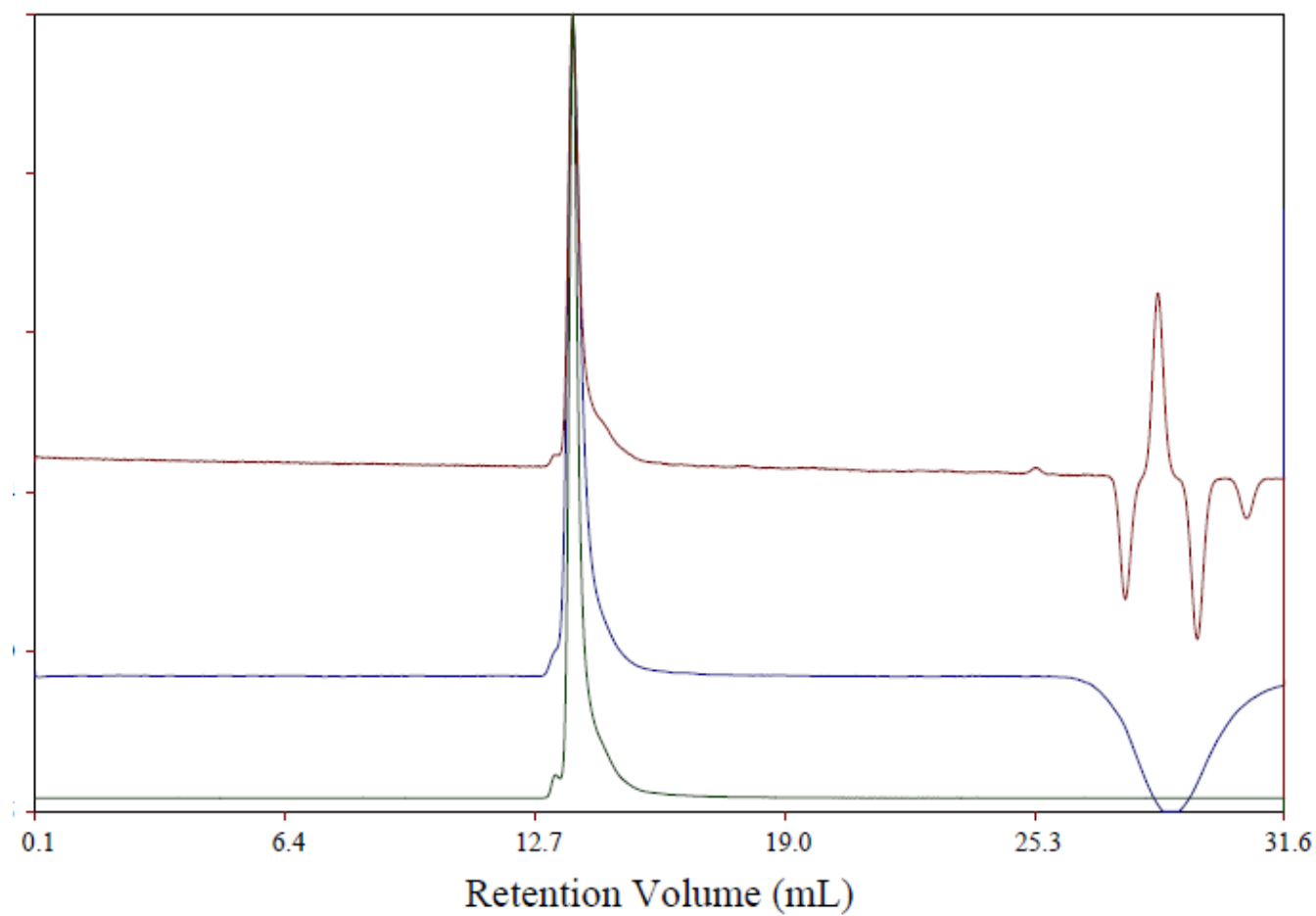


Figure 2. Example of chromatograms for polystyrene standards:

- PSS standards, peak molecular weight $M_p = 67,500$, injected during period 1 (see next tables). From top to bottom at the y intercept, signals correspond to viscometer, refractometer, right-angle laser light scattering.



- PSS standards, $M_p = 2.570.000$, injected during period 1 (see next tables). From top to bottom at the y intercept, signals correspond to refractometer, viscometer, right-angle laser light scattering



- PSS standard, oligomers (see * at bottom of Figure 3), injected during period 2 (see next tables). Only the refractometer trace is displayed (viscometer and light scattering are highly noisy signals because of low molecular weight). Complete characterization of this mixture of oligomers has been achieved by 2D HPLC [3].

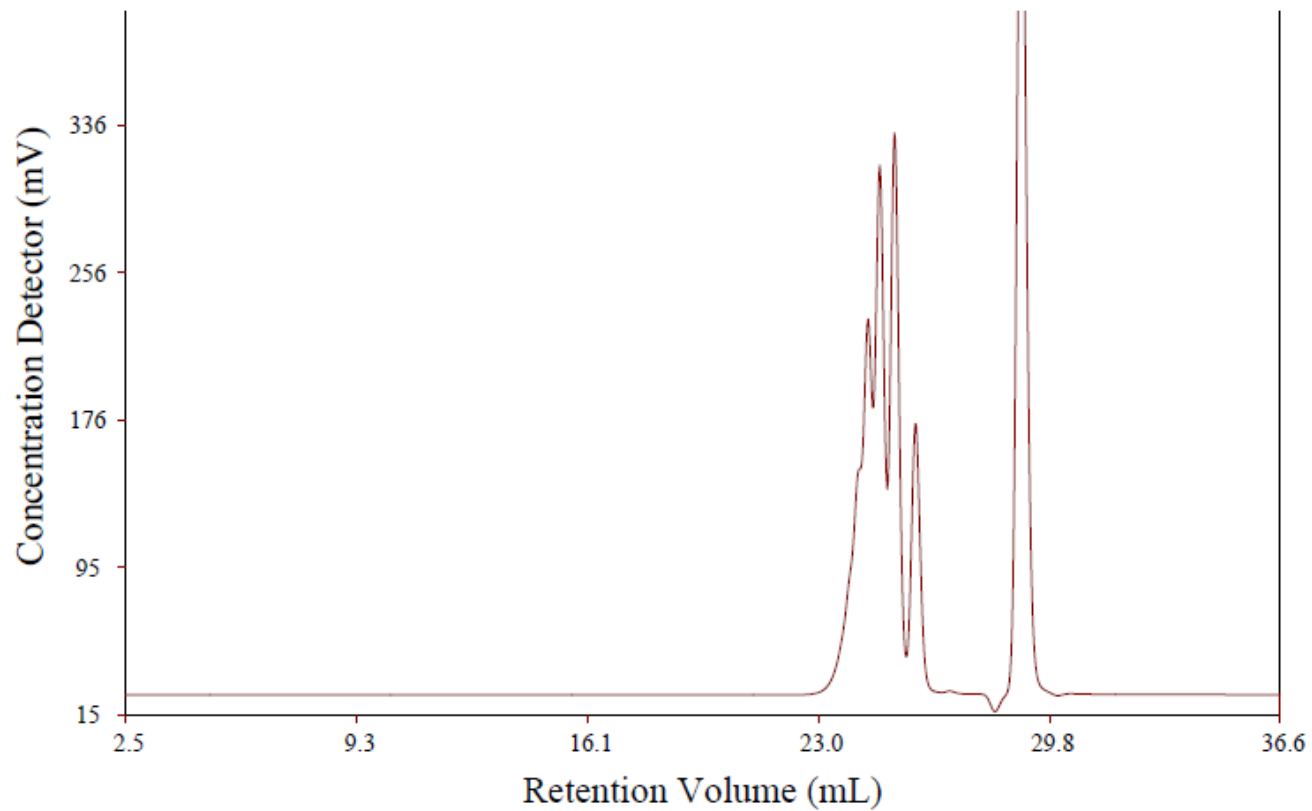
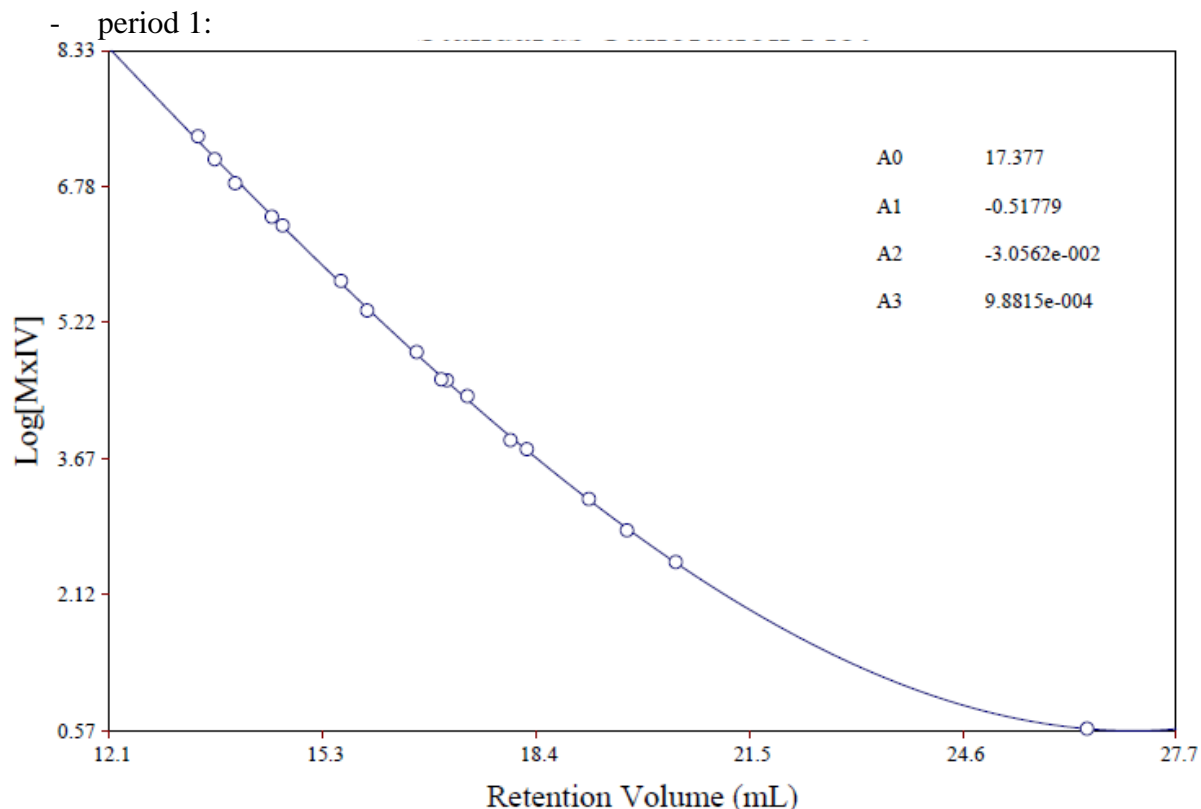


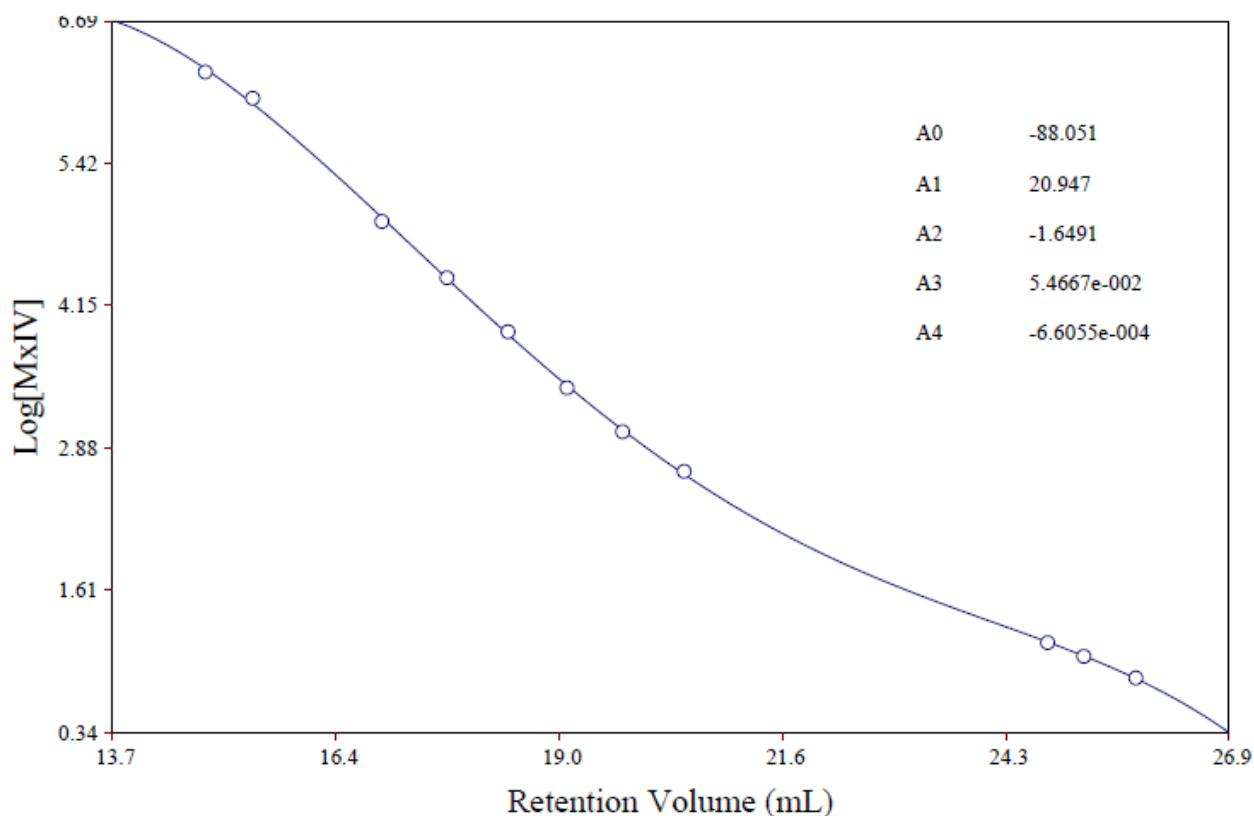
Figure 3. Universal calibration curves obtained at different times of use of the SEC equipment related to this work. IV stands for intrinsic viscosity and A0 to A3 are the fit of the curve by a polynomial function $\log [\eta]M = A_0 + A_1.Vel + A_2.Vel^2 + A_3.Vel^3$. where Vel is the elution volume and $[\eta]M$ is in $dL \cdot mol^{-1}$.



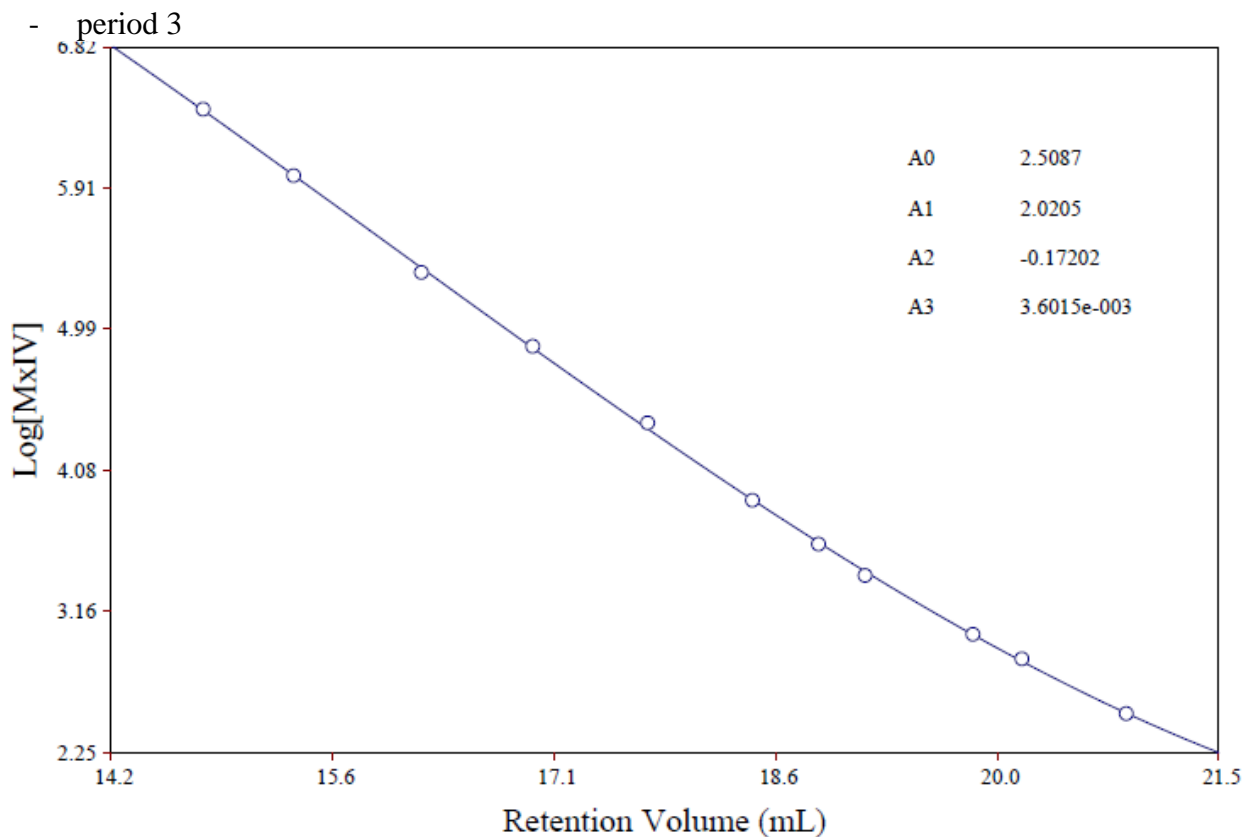
M_p	Elution volume (mL)	Deviation between the fit of the calibration curve and the input M_p (%)
162	26.40	+0.1
4,920	20.40	+1.9
8,390	19.69	-4.9
13,400	19.14	+2.1
29,600	18.23	+2.9
34,800	18.00	-8.7
67,500	17.37	+9.8
89,300	16.99	-7.0

89,300	17.07	+3.6
130,000	16.63	+6.1
246,000	15.90	-5.7
400,000	15.52	+6.5
940,000	14.67	+2.2
1,090,000	14.52	-3.0
1,870,000	13.98	-11.4
2,570,000	13.68	-3.5
3,800,000	13.44	+12.6

- period 2

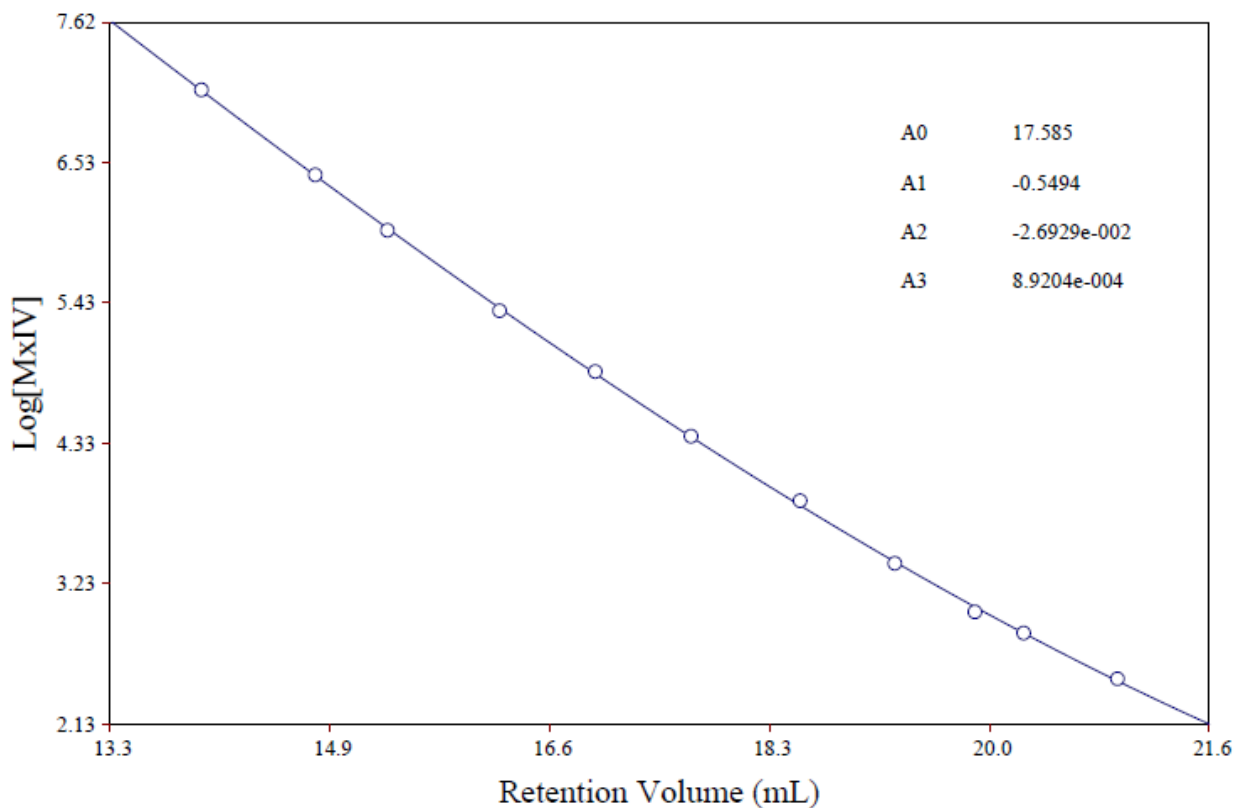


M_p	Elution volume (mL)	Deviation between the fit of the calibration curve and the input M_p (%)
266*	25.81	+1.3
370*	25.20	-0.8
474*	24.77	-1.3
6,040	20.47	+6.1
10,400	19.75	-3.6
18,100	19.09	-4.9
34,800	18.39	+5.5
67,500	17.67	+1.5
130,000	16.90	-7.7
579,000	15.38	+11.9
1,090,000	14.81	-6.3



M_p	Elution volume (mL)	Deviation between the fit of the calibration curve and the input M_p (%)
4,920	20.84	-0.7
8,390	20.16	+3.7
10,400	19.84	+0.6
18,100	19.13	-5.9
24,000	18.83	-2.5
34,800	18.39	-0.9
67,500	17.71	+9.4
130,000	16.95	+2.6
246,000	16.22	-6.6
579,000	15.39	-0.5
1,090,000	14.79	+1.7

- period 4



M_p	Elution volume (mL)	Deviation between the fit of the calibration curve and the input M_p (%)
4,920	20.93	+3.9
8,390	20.22	+0.3
10,400	19.85	-8.6
18,100	19.24	-2.8
34,800	18.52	+8.8
67,500	17.69	+1.2
130,000	16.96	+4.0
246,000	16.23	-4.7
579,000	15.38	-3.5
1,090,000	14.83	+1.4
2,570,000	13.97	+1.2

* The standards whose M_p correspond in fact to a mixture of oligostyrene with butyl and hydrogen as end-groups. The M_p 266, 370, 474, 578 correspond respectively to degrees of polymerization of 2, 3, 4 and 5.

Figure 4: Comparison of the universal calibration curves obtained at different periods

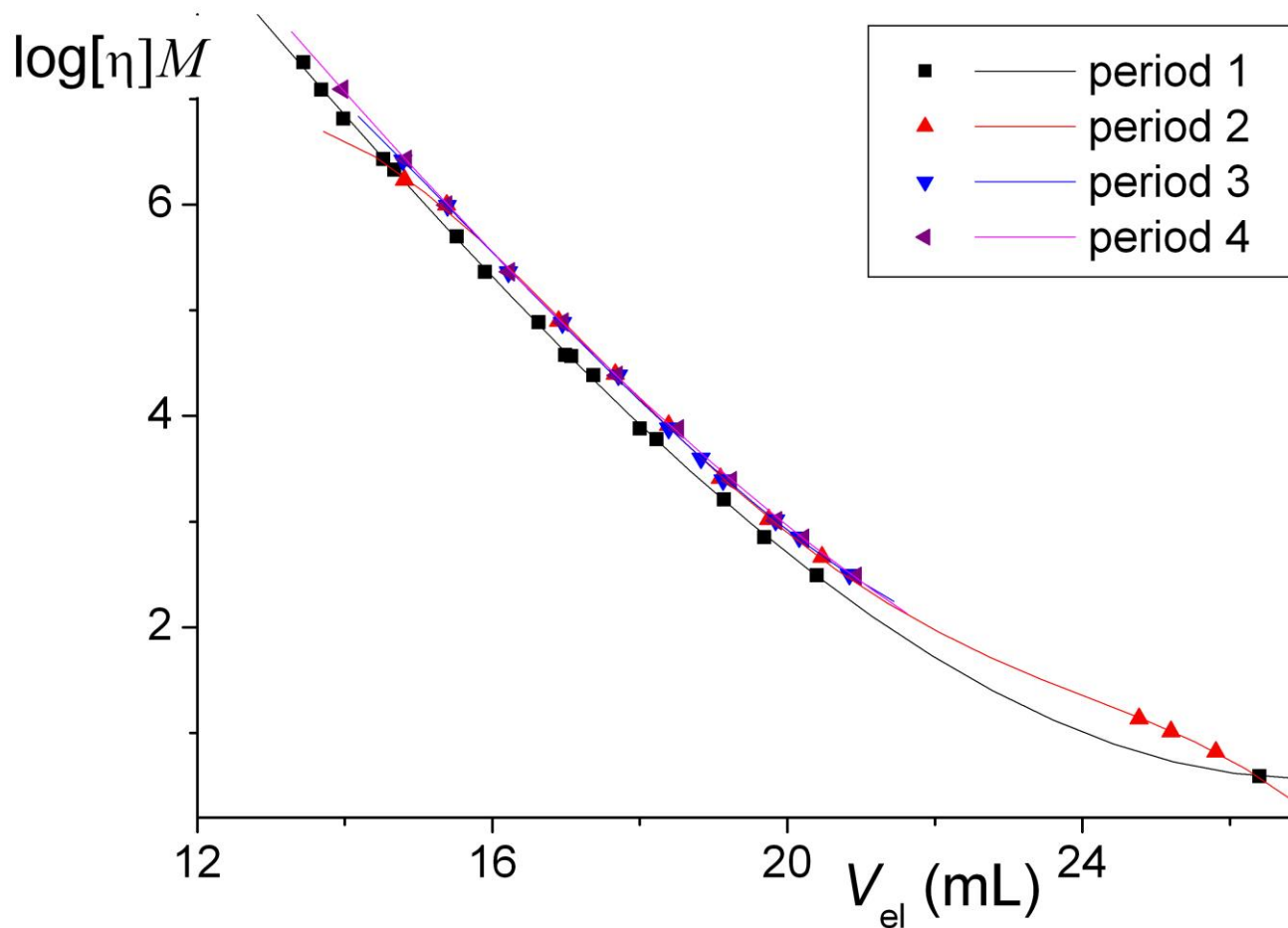


Table 1. Characteristics of the polystyrene standards (PS, PMMA) used to calibrate the multiple detection SEC with the number of time they were used (three calibrations were performed). The final constants were calculated as the arithmetic means of the reasonable values obtained for each standard. Low MWs were not considered for calculation of the average for the calibration of the viscometer and light scattering, while high MWs, i.e. low injection concentrations, were rejected in the case of the refractometer calibration.

<i>Supplier</i>	<i>M_p</i> <i>(g·mol⁻¹)</i> <i>(from supplier)</i>	<i>Polydispersity</i> <i>(from supplier)</i>	<i>Used to calibrate (the number corresponding to the number of times this standard has been used for calibration)</i>		
			<i>Refractometer</i>	<i>Viscometer</i>	<i>Light scattering</i>
PSS	1,620	1.06	1		
PSS	4,920	1.08	2	1	
PSS	8,390	1.04	2	1	
PSS	10,400	1.03	2	2	2
PSS	18,100	1.03			1
PSS	34,800	1.04		1	2
PSS	67,500	1.02	2	2	4
PSS	130,000	1.04	1		6
PSS	246,000	1.06	1		3
PSS	339,000	1.03	1		1
PSS	579,000	1.03	2	1	2
PSS	1,090,000	1.06	1	2	2
PSS	2,570,000	1.04			2
Viscotek	6,040	1.06			
Viscotek	13,400	1.05	1	1	1
Viscotek	29,600	1.03	1	1	1
Viscotek	64,500	1.02			1
Viscotek	89,300	1.04		1	2
Viscotek	170,000	1.04	2	2	2
Viscotek	400,000	1.04	1	1	1
Viscotek	940,000	1.03		1	1
Viscotek	1,870,000	1.07		1	1
Viscotek	3,800,000	1.04		1	1

Table 2. Calibrations constants of the different detectors: the value is as an average on a number of measurements for different standards (injections from different standards were used depending on the detector. Typically, highest molecular weights are not used for the refractometer since they have to be injected at a too low concentration, while lowest molecular weights give too noisy viscometric and light scattering signals). Accuracy is estimated as the ratio of the standard deviation of the measurement to the average constant value. There are two periods (measuring cells for the refractometer and light scattering were changed in-between)

Period	Mass constant (refractometer)			Viscometer constant			Light scattering constant (90°)		
	Value	Accuracy (%)	Number of standards	Value	Accuracy (%)	Number of standards	Value $\times 10^5$	Accuracy (%)	Number of standards
1-3	1824	3.0	8	1090	2.1	12	29.51	2.4	15
4	1162	4.4	8	1063	2.5	8	22.58	5.9	10

Table 3. Peak parameters (skew σ and variance τ for band broadening and offset inter-detector delay corrections) used with Trisec software

Period	Refractometer		Viscometer			Light scattering		
	σ	τ	σ	τ	offset	σ	τ	offset
1-4	0.138	0.121	0.138	0.158	-0.187	0.138	0.094	0.163

Table 4. Benchmark of the triple detector SEC set-up using polystyrene (PS), poly(methyl methacrylate) (PMMA) or poly(*n*-butyl acrylate) (PnBA) standards. After an average period of two months, the set-up was calibrated again following technical problem or just observation that the calibration no longer held. Each period of time given below correspond to one calibration. C is the injection concentration. Diff. is the relative difference between the measured M_p nad the value indicated by the supplier.

- period 1

<i>Polymer (supplier)</i>	<i>C g·L⁻¹</i>	<i>M_p (from supplier)</i>	<i>universal calibration</i>		<i>triple detection</i>		<i>LALLS</i>	
			<i>M_p</i>	<i>Diff.</i>	<i>M_p</i>	<i>Diff.</i>	<i>M_p</i>	<i>Diff.</i>
PS (PSS)	-	18,100	22,000	+19	16,300	-10	15,900	-13
PS (PSS)	5.2	67,500	68,800	+2	69,600	+3	70,900	+5
			66,200	-2	64,200	-5	64,300	-5
			68,200	+1	65,800	-3	64,600	-4
			69,700	+3	64,500	-4,5	63,700	-6
			73,900	+9	62,500	-8	64,300	-4
PS (PSS)	2.1	246,000	272,200	+10	259,800	+5	258,900	+5
PMMA (Interchim)	-	33,700	33,400	-0,1	30,100	-10	29,800	-10

- period 2

<i>Polymer (supplier)</i>	<i>M_p (from supplier)</i>	<i>universal calibration</i>		<i>triple detection</i>		<i>LALLS</i>	
		<i>M_p</i>	<i>Diff.</i>	<i>M_p</i>	<i>Diff.</i>	<i>M_p</i>	<i>Diff.</i>
PS (PSS)	34,800	37,700	+7	32,900	-6	33,800	-3
		37,700	+7	32,700	-6	31,100	-11
PS (PSS)	67,500	73,900	+9	62,500	-8	64,300	-4
PMMA (interchim)	33,700	33,800	+0	32,800	-3	30,500	-10

-period 3

<i>Polymer (supplier)</i>	<i>M_p (from supplier)</i>	<i>universal calibration</i>		<i>triple detection</i>	
		<i>M_p</i>	<i>Diff.</i>	<i>M_p</i>	<i>Diff.</i>
PS (PSS)	67,500	71,800	+6	69,100	+2
		73,300	+8	69,700	+3
		71,400	+6	71,500	+5
		69,400	+3	72,300	+7
		130,000	143,000	+9	118,000
PS (Viscotek)	29,600	34,500	+9	29,400	-1
PnBA (*)	11,700	14,800	+23	11,800	+0
	22,600	30,800	+30	24,300	+7

*: kindly supplied by Dr. Xavier André, University of Bayreuth

- period 4:

Polymer (supplier)	Concentration injection $g \cdot L^{-1}$	M_p (from supplier)	universal calibration		triple detection	
			M_p	Diff.	M_p	Diff.
PS (PSS)	5.2	67,500	68,700	+2	61,500	-9
	-	130,000	133,300	+2	130,000	0
			132,700	+1	129,500	-0
			130,200	+0	122,100	-6
			131,600	+1	127,300	-2
PMMA (Interchim)	-	33,700	37,800	+12	30,700	-9

Table 5. Specific refractive increment, dn/dc , values

- values used in this work for THF at 40 °C for the SEC detectors

Polymer	Poly(ethyl acrylate), PEA	Poly(<i>n</i> -butyl acrylate), PnBA	Poly(2-ethylhexyl acrylate), P2EHA	PS	PMMA
dn/dc ($mL \cdot g^{-1}$)	0.071	0.063	0.073	0.185	0.09
Uncertainty(%)	5	-	5	-	-

These values are arithmetic means of the reasonable values determined on the SEC set-up (poly(ethyl acrylate and poly(2-ethylhexyl acrylate) or available in the literature (poly(*n*-butyl acrylate). and given below.

- dn/dc values for polyacrylates in THF determined in this work or from the literature

Polymer	dn/dc ($mL \cdot mg^{-1}$)	T (°C)	Number of samples (λ in nm)	MW range ($g \cdot mol^{-1}$)	Determination method	Ref.
PEA	0.061 ± 0.002	25	6 (546)	$\bar{M}_w = 7 \cdot 10^4$ to 10^6	RDBP*	[4]
	0.070	30	1 (670)		triple-detection SEC	This work
	0.074	30	1 (670)			
	0.072	30	1 (670)			
	0.072	30	1 (670)			
	0.073	30	1 (670)			
	0.070	30	1 (670)			
	0.076	30	1 (670)			
	0.067	30	1 (670)			
0.075	30	1 (670)				

	0.084	30	1 (670)			
	0.065	40	1 (670)	High conversion by PLP	triple-detection SEC	
	0.067	40	1 (670)			
	0.068	40	1 (670)			
PnBA	0.063 ± 0.002	25	6 (546)			$\bar{M}_w = 3.10^4$ to 10^6
	0.0615	25				[5]
P2EHA	0.068 ± 0.002	25	6 (546)	$\bar{M}_w = 10^5$ to 10^6	RDBP*	[4]
	0.068		4 (546)	$\bar{M}_w = 10^5$ to 10^6	RDBP*	[6]
	0.070	25	1 (436)	$\bar{M}_w = 2 \times 10^6$, $I_p = 1.2$	RDBP*	[7]
	0.079	30	1		triple-detection SEC	This work
	0.073	30	1			
	0.076	30	1			
	0.078	30	1			
	0.076	30	1			
	0.073	30	1			
	0.07	30	1			
	0.068	30	1			
	0.074	30	1			
	0.078	30	1			
	0.069	30	1			
PMMA	0.09					
	0.089	30	(488)			[9]
PS	0.185	30-40			Viscotek	

*RDBP is the Brice-Phoenix differential refractometer.

REFERENCES

- [1] L. Couvreur, G. Piteau, P. Castignolles, M. Tonge, B. Coutin, B. Charleux, J.P. Vairon, *Macromol. Symp.* 174 (2001) 197.
- [2] M. Gaborieau, Solid-state NMR investigation of spatial and dynamic heterogeneity in acrylic pressure sensitive adhesives (PSAs) compared to model poly(n-alkyl acrylates) and poly(n-alkyl methacrylates), PhD thesis, University Louis Pasteur, Strasbourg, France, 2005. <http://www-scd-ulp.u-strasbg.fr/theses/theselec.html>
- [3] M.J. Gray, G.R. Dennis, P.J. Slonecker, R.A. Shalliker, *J. Chromatogr. A* 1073 (2005) 3.
- [4] E. Penzel, N. Goetz, *Angew. Makromol. Chem.* 178 (1990) 191.
- [5] F. Chauvin, A.M. Alb, D. Bertin, P. Tordo, W.F. Reed, *Macromol. Chem. Phys.* 203 (2002) 2029.
- [6] L. Mrkvickova, J. Danhelka, P. Vlcek, *Polym. Comm.* 31 (1990) 416.
- [7] E. Lathova, D. Lath, J. Pavlinec, *Polym. Bull.* 30 (1993) 713.
- [8] J. Brandrup, E.H. Immergut, E.A. Grulke, *Polymer Handbook*, 1999.
- [9] C. Jackson, Y.J. Chen, J.W. Mays, *J. Appl. Polym. Sci.* 61 (1996) 865.